Proinflammatory innate cytokines and metabolomic signatures predict T cell response in active COVID-19

Akshay Binayke[1], Aymaan Zaheer[2†], Jyotsna Dandotiya[1†], Sonu K Gupta[3], Shailendra Mani[3], Manas Tripathi[2], Upasna Madan[1], Tripti Shrivastava[3], Yashwant Kumar[3], Anil K Pandey[4], Deepak K Rathore[3], Amit Awasthi[1,2*]

[1]Immunobiology Lab, Translational Health Science and Technology Institute, Faridabad, India;

[2]Immunology Core, Translational Health Science and Technology Institute, Faridabad, India;

[3]Translational Health Science and Technology Institute, Faridabad, India;

[4]ESIC Medical College and Hospital, Faridabad, India.

*Corresponding author. Email: aawasthi@thsti.res.in

[†] Equal Contribution

Graphical Abstract

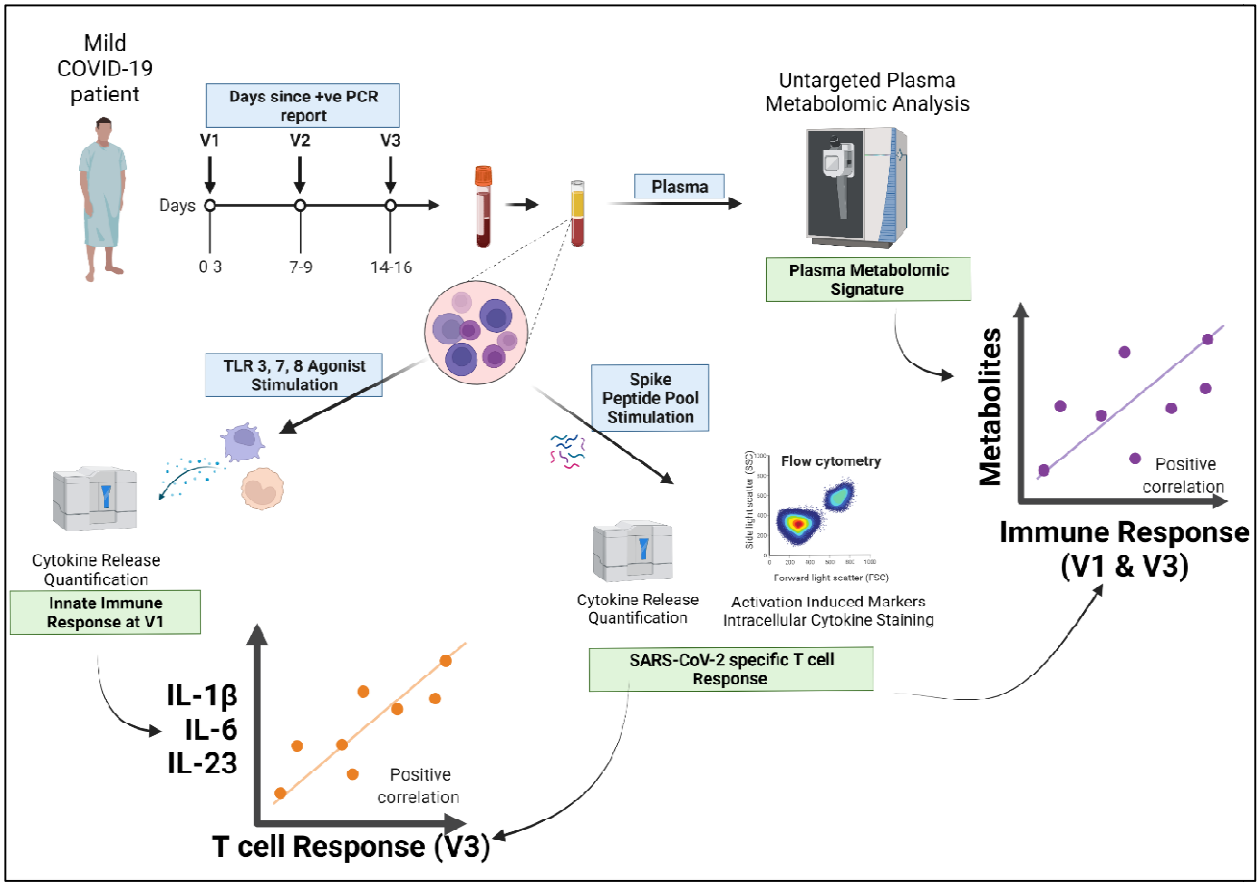

Abstract

The underlying factors contributing to the evolution of SARS-CoV-2-specific T cell responses during COVID-19 infection remain unidentified. To address this, we characterized innate and adaptive immune responses with metabolomic profiling longitudinally at three different time points (0-3, 7-9, and 14-16 days post-COVID-19 positivity) from young mildly symptomatic active COVID-19 patients infected with the ancestral virus in mid-2020. We observed that anti-RBD IgG and viral neutralization are significantly reduced against the Delta variant compared to the ancestral strain. In contrast, compared to the ancestral strain, T cell responses remain preserved against the delta and omicron variants. We determined innate immune responses during the early stage of active infection in response to TLR 3/7/8 mediated activation in PBMCs and serum metabolomic profiling. Correlation analysis indicated PBMCs-derived proinflammatory cytokines, IL-6, IL-1β, and IL-23, and the abundance of plasma metabolites, pyroglutamate, itaconate, and azelaic acid, were predictive of a robust SARS-CoV-

2-specific Th1 response at a later stage (two weeks after PCR positivity). These observations may contribute to designing effective vaccines and adjuvants that promote innate immune responses and metabolites to induce long-lasting anti-SARS-CoV-2 specific T cells response.

Keywords: T cells, Immuno-metabolomics, COVID-19, Vaccine Adjuvant, SARS-CoV-2, Omicron

Key Message:

- Early proinflammatory innate cytokine response is critical for a robust T cell response during COVID-19.
- We report a set of plasma metabolites that significantly correlate with the innate and adaptive immune responses.

INTRODUCTION

T cell immune responses are indispensable in long-lasting protection against the coronavirus disease-19 (COVID-19) (*1-3*). Although variants of concern (VoCs) acquired multiple mutations to evade the humoral immunity generated through vaccination or natural infection or both, T cell immunity remained largely preserved against variants of SARS-CoV-2 (*3-6*). Importantly, memory T cells' response against SARS-CoV-2 persists for a long time since antigen exposure and thus protects from severe infection upon re-exposure to SARS-CoV-2 and its variants (*7*). The frequency and magnitude of antigen-specific T cell response could potentially affect the clinical manifestations of COVID-19 (*8-10*). Therefore, it is critical to understand the factors that shape the magnitude of T cell responses during SARS-CoV-2 infections.

Antigen-presenting cells (APCs) provide secondary signals in the form of cytokines that are critical in modulating the T cell activation and differentiation (*11*). However, the phenotype of cytokines secreted by innate immune cells in generating a comprehensive T cell response is not clearly understood in COVID-19. Systems biology studies have shown that proinflammatory cytokines, IL-6, IL-1β, and TNF-α, originating from the SARS-CoV-2 infected lungs, but not from the peripheral blood cells, contribute to COVID-19 severity (*12*). Therefore, studying the systemic levels of cytokines to predict the T cell response may prove misleading. There are limited reports of cellular innate immune responses and their correlation with adaptive immunity. Few recent longitudinal studies have documented the early innate and adaptive immune responses during mild COVID-19 (*13, 14*); however, no reports identify a correlation of an early innate immune response with the generation of T cell response in active COVID-19. To address this, we used TLR 3, 7, and 8 agonists to stimulate PBMCs isolated within three days of PCR diagnosis of mild-COVID-19 patients and measured the range and magnitude of innate cytokine release, which were further correlated with the evolution of virus-specific T cell response during active COVID-19.

Since an extensive interplay is reported between plasma metabolites and immune cell activation in COVID-19 patients (*15-19*), metabolic analysis in the plasma samples of longitudinal active COVID-19 patients pointed out a set of metabolites significantly correlate with the innate and adaptive immune responses.

Our results reveal that the antiviral TLR-specific proinflammatory cytokine activity by PBMCs, along with a plasma metabolic signature, works in a coordinated fashion to generate a robust T cell immune response against COVID-19 infection.

MATERIALS AND METHODS

Human Ethics: All the experiments were performed according to the suggested guidelines of the Institutional Ethics Committee (Human Research) of THSTI and ESIC Hospital, Faridabad (Letter Ref No: THS 1.8.1 (97) dated 07th July 2020). Human blood samples were collected from COVID-19 patients and healthy individuals after the written informed consent. Individuals were enrolled in this study based on the inclusion/exclusion criteria prescribed by the Institutional Ethics Committee (Human Research) of THSTI.

THSTI In-house RBD IgG ELISA:

ELISAs to detect IgG binding to RBDs were performed as previously described (*20*). A positive convalescent and negative control sample were added to each plate for normalization. The assay results were normalized by dividing the blank subtracted readings of each sample by negative control to obtain the fold change reading.

Virus Neutralization Assay:

Virus microneutralization assay titers were estimated as described previously (*12*). Briefly, plasma samples were serially diluted from 1/20 to 1/2560 and incubated with the wildtype and the delta SARS-CoV-2 isolates. 50% neutralization values were estimated with four-parameter logistic regression.

Peptide Pool: 15mers peptide pools with an overlap of 11 amino acids spanning the entire sequence of Spike protein (157+158 peptides, JPT, PepMix, Cat. No.PM-WCPV-S-1 (Ancestral), PM-SARS2-SMUT06-1 (Delta) and PM-SARS2-SMUT08-1 (Omicron)) were used for the determining the WT, B.1.617.2 and B.1.1.529 SARS-CoV-2-spike specific T-cell responses by AIM assay, ICS and cytokine bead assay.

SARS-CoV-2 Specific T cell response: SARS-CoV-2 Specific T cell responses were studied as described previously (*6, 21, 22*). Spike-specific cytokine production was background-subtracted by the values obtained with the DMSO-containing medium. Negative values were set to the Limit of detection. The stimulation index (SI) was calculated by dividing the frequency of AIM+ CD4 or CD8 cells recorded in stimulated wells by the unstimulated wells.

Metabolomic Analysis: Metabolomic profiling of plasma metabolites was performed as described previously (*23-26*). The LC/MS obtained data were processed using the Progenesis QI for metabolomics (Nonlinear dynamics, a Waters Company) software using the default setting. Manual processing of the raw data by removing drugs and exposome metabolites led to the identification of 176 metabolites at all three-time points. All the statistical and functional analysis, including the PCA, heat map, pathway enrichment analysis, PLS-DA, and analysis of variance (ANOVA), was done based on the observed peaks intensity using the online open-source software Metaboanalyst 5.0. Before analysis, a data integrity check was performed, and the raw data were normalized by sum, log-transformed, and scaled by Pareto scaling. The volcano plots were constructed using the online available package VolcaNoseR (*27*).

In vitro stimulation of PBMCs with TLR agonists:

PBMCs were stimulated as previously described (*12*), with some modifications. Approximately one million cells were added to each well, and all wells received stimulation with a viral cocktail containing 4.0 μg/ml R848 and 25 μg/ml poly I:C. Negative control DMSO stimulated cells were also cultured for each sample. The cells were incubated in a 5% CO2 incubator at 37ºC for 24 hours, after which supernatant was collected for analysis of cytokine secretion.

Analysis of Cytokine Secretion by Luminex:

Cytokine secretion in the cell culture supernatant was analyzed with a customized Premixed Multi-Analyte Luminex Discovery Assay kit (LXSAHM-10 (peptide pools stimulation); LXSAHM-15 (TLR agonist stimulation), R&D systems). The assays were performed as per the manufacturer's instructions. The analytes examined upon peptide pool stimulation were Granzyme B, IL-2, IL-5, IL-12 p70, IL-23, IFN-gamma, IL-4, IL-6, IL-17/IL-17A, and TNF-alpha.

Data Representation and Analysis:

The statistical analysis and data representation was performed using GraphPad Prism 9.0 and FlowJo XV. Unless otherwise stated, Mann Whitney Test and Wilcoxon matched-pairs signed-rank tests were employed for unpaired and paired comparisons, respectively. All the correlation analyses were performed using the Pearson correlation test. The cytokine secretion response

upon peptide or TLR stimulation was calculated as fold change data for the correlation analysis by dividing the stimulated wells by unstimulated wells of the same sample. Those metabolites belonging to V1 and V3 that significantly correlated ($p<0.05$, $r>0.5$) with the proinflammatory adaptive immune responses and/or TH1 skewed T cell immune responses and has pathway library of KEGG were selected for Pathway Analysis using the Metaboanalyst 5.0 software (*28*). The graphical abstract was prepared using Biorender.com.

RESULTS

IgG and IgM response against RBD protein of WT and VoCs of SARS-CoV-2

To investigate the factors that contribute to the priming of a robust anti-SARS-CoV-2 T cell response, we longitudinally studied immune-metabolomic signatures during acute infection in young mildly symptomatic COVID-19 patients who get infected with the ancestral virus in mid-2020 by collecting blood samples on day 0-3 (indicated as " V1"), day 7 (indicated as "V2") and day 14 (indicated as "V3") from the date of PCR positive infection report. Clinically relevant medical information (e.g., age, patient-reported symptoms) was collected at the time of enrolment. For comparison, blood was also collected from age-matched SARS-CoV-2 RT-PCR negative healthy volunteers (**Table S1**). The clinical cohort was considerably young and consisted of 8 females and 13 males with a median age of 28 years (IQR: 25:34) (**Table S1**). From the collected blood samples, we separated the plasma and PBMCs, which were cryopreserved until further experimentation. The humoral immune response against SARS-COV-2 and its variants was evaluated using the plasma samples collected from the 21 patients. PBMCs from all three-time points were used to determine antigen-specific T cell response dynamics during acute COVID-19. To study the status of innate immunity against SARS-COV-2, we *ex vivo* stimulated the PBMCs of V1 samples with a cocktail of TLR 3/7/8 agonists, and the released cytokines were quantified. We performed a Pearson correlation analysis of the innate immune response from V1 samples and compared them with the SARS-CoV-2 specific T cell immune response of V3. The metabolic signature obtained from the plasma was further correlated with the SARS-CoV-2 specific innate and T cell immune responses (**Fig. 1A**).

To study the kinetics of the antibody response against the SARS-CoV-2, we first investigated the IgG response against the SARS-CoV-2 RBD protein using Enzyme-linked immunosorbent assays (ELISAs). Anti-RBD (ancestral) IgG was increased significantly (in 85% of the patients) such that the median relative fold change of IgG response increased three-fold by V2 and V3 compared to V1 (**Fig. 1B**). Anti-RBD IgG response was found to be decreased against delta compared to ancestral RBD proteins, as indicated by their ratio (**Fig. 1C-E**). While the median NAb titers increased significantly by V2 and V3 as compared to V1 against the ancestral virus (**Fig. 1F**), NAb titers against the delta were found to be considerably decreased at V2 and V3 as

compared to the ancestral virus ($p<0.0001$, **Fig. 1H**). We observed that even by V3, only 33% (7/21) individuals had detectable levels of NAbs against the Delta variant (**Fig. 1G**), suggesting that the humoral immune protection against VoCs in active COVID-19 patients infected with ancestral strain is broadly inadequate.

Spike-specific T cell response in COVID-19 patients:

Next, we studied the initiation of the antigen-specific T cell response against ancestral, delta, and omicron from the PBMCs of active COVID-19 patients infected with ancestral SARS-CoV-2 virus in mid-2020, during the first wave of the pandemic. T cells response was measured after stimulating PBMCs with peptide pools spanning the entire length of the spike protein for 20-24h and calculating the expression of activation-induced markers (AIM) (*10*) and Th1 cytokine secretion and intracellular live-cell flow cytometry (*29*).

The AIM+ in CD4+ T cells was observed as early as V1 (6/21), which may be attributed to pre-existing cross-reactive T cells from prior common cold coronavirus infections (*30*). The magnitude of SARS-CoV-2-specific CD4+ T cells increased significantly by V2 (day 7, $p = 0.0027$) and by V3 (day 14, $p = 0.0028$) (**Fig. 2 A-B**). Consistent with the previous reports (*10*), the AIM+ cells in CD4+ T cells were observed in ~76% of the patients by V3 (16/21). Likewise, AIM+ spike-specific CD8+ T cells were detected as early as V1 (4/21). Interestingly, unlike CD4+ T cells, the frequency and magnitude of AIM+ cells in CD8+ T cells peaked quickly by V2 ($p = 0.021$) and did not change significantly by V3 ($p = 0.52$) (**Fig. 2 C-D**). Notably, antigen-specific CD8+ T cells were detected in only 57% (12/21) of the patients, in line with the previous findings reported by Moderbacher et al., 2020 (*10*).

Intracellular cytokine staining of spike peptide pool stimulated PBMCs showed an IFNγ dominated CD4+ and CD8+ T cell response with intracellular IFN gamma expression significantly increasing from V1 to V3 (**Fig. 2G-L).** Cytokine secretion analysis of culture supernatant confirmed a steady increase in the secretion of cytokines such as IFN-γ, TNFα, and IL-2 (**Fig. 3A-C**), whereas Th-2 and Th-17 specific cytokines did not change significantly (**Fig. 2G, J; Fig. 3 D, E, G**). The cytotoxic response, evaluated by the expression of Granzyme B, increased extensively by 14 days after virus detection (**Fig. 3I**).

To sum up, the SARS-CoV-2 specific T cell immune responses were predominated by interferon expression, and their magnitude progressively increased with the advent of time since antigen exposure.

T cell response against ancestral, delta, and omicron is largely preserved in active COVID-19 patients

We found that the T cell response evolves and increases at 14 days post COVID-19 infection with the ancestral strain. To confirm whether T cell response elicited by the ancestral strain in active COVID-19 patients could cross-react with the delta and omicron spike protein, we tested and compared the T cell response in the PBMCs (n=24) of active COVID-19 patients from V2 and V3 against the spike peptide pools of the ancestral, delta, and omicron variants (**Fig. 4**). We observed that the T cell response is largely preserved with a slight reduction against delta (1.3-fold) and the omicron (1.5-fold) spike protein compared to the ancestral spike protein. Compared to the ancestral response, the geometric mean of the AIM+ in CD4+ response was reduced by 31% against delta (p=0.0162) and 58% against Omicron spike (p=0.0005) (**Fig. 4A**). However, the functional profile remained broadly comparable among the variants (**Fig. 4 B-D**). We also did not find any significant differences between the functionality of the antigen-specific T cells as determined by the expression of intracellular cytokines such as IFN-γ, IL-2, and TNFα (**Fig. 4 E**). A pairwise comparison further revealed that the CD4+ AIM response was preserved entirely in 30% of samples stimulated with delta spike peptides and 15% stimulated with the omicron spike peptides (**Fig. 4 F, G**).

The geometric mean antigen-specific CD8+ AIM response was reduced by 3 to 5 fold in the delta and omicron variants, respectively (**Fig. 4 H**). However, the functional phenotypes of the antigen-specific CD8 T cells were similar among the VoCs compared to the ancestral spike antigen (**Fig. 4 I-K**). The pairwise comparison further revealed a maximum reduction in 66% of individuals against the spike of delta variant and 75% against the spike of omicron variant (**Fig. 4 L, M**).

Taken together, although the humoral immune response is abrogated against the VoCs in actively infected individuals, the cellular immune responses persist. Our results imply the importance of

the cellular immune responses against COVID-19. Thus it is essential to understand further what factors determine the generation of a robust T cell response during active COVID-19.

Early proinflammatory innate cytokine response correlates with a robust T cell response

For the differentiation and activation of functional T cells, the antigen-presenting cells (APCs) must provide three signals to the T cells. One is via direct TCR-MHC interaction, the second is through cognate interaction of adhesion molecules, and the third is by cytokine signaling (*11*). Therefore, the APCs play a critical role in shaping the T cell response during exposure to a foreign antigen. Given the earlier findings that COVID-19 infection impairs the APCs such as the pDCs and myeloid cells (*12, 31*), we wanted to test what functional phenotype of APCs correlates with the virus-specific T cell responses. We performed *ex vivo* stimulation of V1 PBMCs of our COVID-19 cohort with a cocktail of synthetic agonists of toll-like receptor (TLR) 3, 7, and 8, which are known to sense virus-derived molecules and initiate an antiviral response (*32*). In the presence and absence of the TLR agonists cocktail of poly I:C (TLR3) and R848 (TLR 7/8), the PBMCs were cultured for 24h as described previously (*12*). The fold change in cytokine expression of TLR stimulated samples compared to the unstimulated wells was correlated with the stimulation indices of T cell response elicited in V3 (**Fig. 5A**).

The Pearson correlation analysis showed that the PBMCs from individuals that secreted a heightened proinflammatory cytokine response in the form of IL-6, IL-1β, and IL-23 upon TLR stimulation correlated significantly with the spike-specific T cell immune response in the form of the secretion of IFN-γ, TNFα, and Granzyme B (GZB) (**Fig. 5B**). In contrast, the remaining cytokines such as IFN-γ, IL-12p70, CCL2, and IL-10 did not correlate. Moreover, the proinflammatory cytokines did not associate with non-Th1 cytokines such as IL-5, and IL-17 (**Fig. 5B**). To sum up, individuals exhibiting a proinflammatory functional phenotype of innate immune cells during the early stages of infection subsequently tend to develop a robust antiviral T cell immunity.

Distinct Metabolomic Alterations characterize acute COVID-19 infection

To obtain a broad view of the metabolic status, we studied the longitudinal plasma metabolite profile in our cohort of 21 COVID-19 patients and compared them with the plasma of 12 healthy volunteers (**Table S1**). The plasma samples from V1 and V3 were processed for UHPLC-

MS/MS analysis, and 240 different metabolites were identified. These 240 metabolites were further screened to remove drugs and other artificial compounds and derivatives to obtain 176 metabolites. Unsupervised PCA analysis of the metabolites in our patient cohort displayed a clear distinction that separated the control (healthy individuals), COVID-19 early time point (V1), and late time point (V3) individuals (**Fig. 6A**). The Partial Least Squares – Discriminant Analysis (PLS-DA) was employed to identify the top-15 important metabolites across the three different groups (**Fig. 6B**). Moreover, hierarchical clustering of the top 50 metabolites showed a notable shift in the metabolic signature among acute COVID-19 patients compared to the healthy individuals (**Fig. 6 C**). The PLS-DA and hierarchical clustering analysis pointed out that the levels of metabolites and derivatives of the Citric Acid cycle, such as Citrate, Itaconate, and trans-aconitate, were significantly reduced in COVID-19 patients (**Fig. 6B-C**). In contrast, metabolites such as glutamic acid derivatives – Pyroglutamate and N-methyl-L-glutamic acid were enriched in the plasma of COVID-19 patients (**Fig. 6B-C**). Of the 176 metabolites, 158 were significantly differentiated in COVID-19 patients (FDR<0.001), exhibiting a distinct metabolic profile. Pathway enrichment analysis using the KEGG database showed the metabolites involved in the Phenylalanine metabolism, Arginine and Proline metabolism, etc., were significantly altered during COVID-19 (**Fig. 6E**). Compared to V1, 33 metabolites were significantly down and 13 significantly up (p=0.001, FC>1.5, **Fig. 6D**) during V3.

To understand the immune-metabolomic interaction, we performed a Pearson correlation of metabolites with the innate and adaptive immune responses in COVID-19 patients and shortlisted the significantly correlating metabolites (r>0.5, p<0.05). Pathway analysis of plasma metabolites that significantly correlated with the innate immune response from V1 and the T cell immune response from V3 samples showed that the metabolites involved in arginine biosynthesis, histidine metabolism, alanine-aspartate, and glutamate metabolism were enriched in plasma samples from V1 as well as V3 (**Fig. 7 A-B**). Notably, the metabolites such as pyroglutamate, itaconate, and norvaline which are involved in the glutathione metabolism, citrate cycle, and amino acid biosynthesis, correlated significantly with the early and late-stage immune responses (**Fig. 7**).

DISCUSSION

No other viral disease in the history of humanity has been studied and reported to the extent of COVID-19. And neither has any disease in recent history caused the socio-economic devastation of life on such a global scale (*33*). Several integrative studies have attempted to understand the immune correlates of protection against COVID-19 (*34-36*). These studies have shown that the late Induction of T cell responses (*37*), impaired type I interferon response (*38, 39*), and weakened innate immune responses are immune hallmarks of severe COVID-19 (*12, 34*).

In this study, the samples were collected during the first wave of COVID-19 (between 07th July and 04th September 2020) before the existence of delta, and omicron VoCs, which allowed us to determine how T cells primed with the ancestral strain react with spike antigen of delta and omicron variants. The magnitude of antigen-specific T cell response against the ancestral spike was similar to the previous reports (*7, 10*). Furthermore, we observed that the T cell response elicited during the active ancestral SARS-CoV-2 infection persists but is relatively reduced against the delta and omicron variants compared to the ancestral spike. The extent of reduction in the magnitude of T cell response against VoCs is more prominent in our cohort than in previous reports in vaccinated individuals (*4, 5, 40*). Such observation could be because the overall magnitude of T cell response is low in acute samples (*7*) and, therefore, may have resulted in a limited scope for cross-reactivity against the VoCs.

Given the importance of T cell responses in limiting disease severity and protection against emerging variants, the next generation of vaccines must primarily focus on the magnitude of T cell responses generated upon vaccination. However, limited studies have investigated the factors contributing to robust T cell immune responses during COVID-19. An integrative research reports that type I interferon response does not correlate with the antiviral T cell responses (*14*). In contrast, another combinatorial study reported a temporary increase of IFN-β and IP10/CXCL10 levels associated with a dominant SARS-CoV-2-specific CD4 T cell response (*13*). However, none of these combinatorial reports studied the TLR-specific functional innate immune response, which is more virus-specific and functional in nature (*12*).

Increased plasma IL-6, TNF-a, and IL-1β are characteristic of severe COVID-19 patients (*41*). However, it has now been well established that the source of these proinflammatory cytokines is

not the innate immune cells but the non-immune host tissues such as lungs (*12*). Furthermore, in severe COVID-19, the innate cell expression of these proinflammatory cytokines is instead significantly reduced (*12*). Our investigation of innate and T cell response across the early stages of infection showed that the PBMCs from individuals with a strong proinflammatory innate immune response also exhibit a robust T cell response against SARS-CoV-2 infection. The correlation of proinflammatory Th17 differentiating cytokines, IL-23, IL-1β, and IL-6 (*42*), with the Th1 response in the later stages of the disease needs further investigation. Interestingly, we recently reported that IL-17A transcripts were higher at the early stage (2-4 days post-infection) of SARS-CoV-2 infection in hamsters (*43*). Therefore, it may be interesting to investigate further if there is any Th1/Th17 plasticity (*44*) that may play a role in the development of T cell response during COVID-19. Such investigations are fundamental for designing adjuvants that trigger a robust and long-lasting memory T cell immunity.

There is an orchestrated symphony between the metabolism and immune responses where both players harmonize (*45*). Although other groups have reported the longitudinal metabolomic signature (*46*) and single-cell transcriptomic landscape in COVID-19 patients (35), no study correlated the functional innate and T cell response with the metabolic landscape. Our analysis found a significant correlation between the SARS-CoV-2 specific immune responses and the metabolites involved in pathways such as arginine biosynthesis; citrate, histidine, and glutamine/glutamate metabolism. The immunomodulatory effects of L-Arginine (*46*), Norvaline (*47*), Itaconate (*48-50*), and Azelaic Acid (*51, 52*) have been reported independently or in the context of disease pathogenesis. Enrichment of these metabolites as correlative markers of anti-SARS-CoV-2 immune responses further underlines their importance in immunomodulatory mechanisms. To conclude, our study highlights the importance of T cell response against the emerging variants of SARS-CoV-2. We show how the PBMC-derived innate responses are critical for generating a robust T cell response; however, how the metabolites could act as potential immunomodulator needs further examination.

Acknowledgment:

We acknowledge the funding through the Mission COVID Suraksha grant (BT/CS0010/CS/02/20) – from BIRAC, Department of Biotechnology, for enabling this study. We thank all the volunteers who donated their blood samples for this study. We sincerely thank the staff and students of the Translational Health Science and Technology Institute (THSTI; Faridabad, India) for helping to ensure the smooth conduct of the study.

Author contributions:

Conceptualization: AA, DR, AB

Methodology: AB, AZ, JD, YK, SG, UM, SM, MT, TS

Investigation: AA, DR, SM, YK, TS

Visualization: AB

Funding acquisition: AA, DR, AB

Project administration: AB, DR

Supervision: AA, DR

Writing – original draft: AB, AZ, AA

Writing – review & editing: AA

Competing interests: Authors declare that they have no competing interests.

Reference

1. D. S. Stephens, M. J. McElrath, COVID-19 and the Path to Immunity. *JAMA* **324**, 1279-1281 (2020).
2. N. Sherina *et al.*, Persistence of SARS-CoV-2-specific B and T cell responses in convalescent COVID-19 patients 6-8 months after the infection. *Med (New York, N.Y.)* **2**, 281-295.e284 (2021).
3. A. Grifoni *et al.*, SARS-CoV-2 human T cell epitopes: Adaptive immune response against COVID-19. *Cell host & microbe* **29**, 1076-1092 (2021).
4. Y. Gao *et al.*, Ancestral SARS-CoV-2-specific T cells cross-recognize the Omicron variant. *Nature Medicine*, (2022).
5. R. Keeton *et al.*, T cell responses to SARS-CoV-2 spike cross-recognize Omicron. *Nature* **603**, 488-492 (2022).
6. A. Tarke *et al.*, SARS-CoV-2 vaccination induces immunological T cell memory able to cross-recognize variants from Alpha to Omicron. *Cell* **185**, 847-859.e811 (2022).
7. N. Le Bert *et al.*, SARS-CoV-2-specific T cell immunity in cases of COVID-19 and SARS, and uninfected controls. *Nature* **584**, 457-462 (2020).
8. J. L. Schultze, A. C. Aschenbrenner, COVID-19 and the human innate immune system. *Cell* **184**, 1671-1692 (2021).
9. D. Mathew *et al.*, Deep immune profiling of COVID-19 patients reveals distinct immunotypes with therapeutic implications. *Science* **369**, eabc8511 (2020).
10. C. Rydyznski Moderbacher *et al.*, Antigen-Specific Adaptive Immunity to SARS-CoV-2 in Acute COVID-19 and Associations with Age and Disease Severity. *Cell* **183**, 996-1012.e1019 (2020).
11. R. Dalal, S. Sadhu, A. Awasthi, in *Translational Autoimmunity*, N. Rezaei, Ed. (Academic Press, 2022), vol. 1, pp. 93-121.
12. P. S. Arunachalam *et al.*, Systems biological assessment of immunity to mild versus severe COVID-19 infection in humans. *Science* **369**, 1210-1220 (2020).
13. C. M. Capelle *et al.*, Combinatorial analysis reveals highly coordinated early-stage immune reactions that predict later antiviral immune responses in mild COVID-19 patients. *Cell Reports Medicine*.

14. A. Chandran *et al.*, Rapid synchronous type 1 IFN and virus-specific T cell responses characterize first wave non-severe SARS-CoV-2 infections. *Cell Reports Medicine* **3**, 100557 (2022).
15. J. W. Lee *et al.*, Integrated analysis of plasma and single immune cells uncovers metabolic changes in individuals with COVID-19. *Nature Biotechnology* **40**, 110-120 (2022).
16. A. F. Rendeiro *et al.*, Metabolic and Immune Markers for Precise Monitoring of COVID-19 Severity and Treatment. *Frontiers in Immunology* **12**, (2022).
17. S. M. O'Carroll, L. A. J. O'Neill, Targeting immunometabolism to treat COVID-19. *Immunotherapy Advances* **1**, (2021).
18. C. N. Khwatenge, M. Pate, L. C. Miller, Y. Sang, Immunometabolic Dysregulation at the Intersection of Obesity and COVID-19. *Frontiers in Immunology* **12**, (2021).
19. P. J. Siska *et al.*, Metabolic imbalance of T cells in COVID-19 is hallmarked by basigin and mitigated by dexamethasone. *The Journal of Clinical Investigation* **131**, (2021).
20. S. Chaudhuri *et al.*, Comparative evaluation of SARS-CoV-2 IgG assays in India. *Journal of Clinical Virology* **131**, 104609 (2020).
21. R. Thiruvengadam *et al.*, Effectiveness of ChAdOx1 nCoV-19 vaccine against SARS-CoV-2 infection during the delta (B.1.617.2) variant surge in India: a test-negative, case-control study and a mechanistic study of post-vaccination immune responses. *The Lancet Infectious Diseases*, (2021).
22. J. M. Dan *et al.*, Immunological memory to SARS-CoV-2 assessed for up to 8 months after infection. *Science* **371**, eabf4063 (2021).
23. S. Naz *et al.*, Development of a Liquid Chromatography–High Resolution Mass Spectrometry Metabolomics Method with High Specificity for Metabolite Identification Using All Ion Fragmentation Acquisition. *Analytical Chemistry* **89**, 7933-7942 (2017).
24. A. Kumar *et al.*, Metabolomic analysis of primary human skeletal muscle cells during myogenic progression. *Scientific Reports* **10**, 11824 (2020).
25. S. Sadhu *et al.*, Gefitinib Results in Robust Host-Directed Immunity Against Salmonella Infection Through Proteo-Metabolomic Reprogramming. *Frontiers in Immunology* **12**, (2021).

26. Z. A. Rizvi *et al.*, High-salt diet mediates interplay between NK cells and gut microbiota to induce potent tumor immunity. *Science Advances* **7**, eabg5016 (2021).
27. J. Goedhart, M. S. Luijsterburg, VolcaNoseR is a web app for creating, exploring, labeling and sharing volcano plots. *Scientific Reports* **10**, 20560 (2020).
28. J. Chong *et al.*, MetaboAnalyst 4.0: towards more transparent and integrative metabolomics analysis. *Nucleic acids research* **46**, W486-W494 (2018).
29. U. Sahin *et al.*, COVID-19 vaccine BNT162b1 elicits human antibody and TH1 T cell responses. *Nature* **586**, 594-599 (2020).
30. A. Grifoni *et al.*, Targets of T Cell Responses to SARS-CoV-2 Coronavirus in Humans with COVID-19 Disease and Unexposed Individuals. *Cell* **181**, 1489-1501.e1415 (2020).
31. M. S. Diamond, T.-D. Kanneganti, Innate immunity: the first line of defense against SARS-CoV-2. *Nature Immunology* **23**, 165-176 (2022).
32. A. M. Krieg, J. Vollmer, Toll-like receptors 7, 8, and 9: linking innate immunity to autoimmunity. *Immunological reviews* **220**, 251-269 (2007).
33. L. S. Flor *et al.*, Quantifying the effects of the COVID-19 pandemic on gender equality on health, social, and economic indicators: a comprehensive review of data from March, 2020, to September, 2021. *The Lancet*, (2022).
34. A. J. Wilk *et al.*, Multi-omic profiling reveals widespread dysregulation of innate immunity and hematopoiesis in COVID-19. *Journal of Experimental Medicine* **218**, (2021).
35. E. Stephenson *et al.*, Single-cell multi-omics analysis of the immune response in COVID-19. *Nature Medicine* **27**, 904-916 (2021).
36. D. Barh *et al.*, A novel multi-omics-based highly accurate prediction of symptoms, comorbid conditions, and possible long-term complications of COVID-19. *Molecular Omics* **17**, 317-337 (2021).
37. A. T. Tan *et al.*, Early Induction of functional SARS-CoV-2-specific T cells associates with rapid viral clearance and mild disease in COVID-19 patients. *Cell Reports* **34**, 108728 (2021).
38. J. Hadjadj *et al.*, Impaired type I interferon activity and inflammatory responses in severe COVID-19 patients. *Science* **369**, 718-724 (2020).

39. Z. Wang, H. Pan, B. Jiang, Type I IFN deficiency: an immunological characteristic of severe COVID-19 patients. *Signal Transduction and Targeted Therapy* **5**, 198 (2020).
40. J. Liu *et al.*, Vaccines elicit highly conserved cellular immunity to SARS-CoV-2 Omicron. *Nature* **603**, 493-496 (2022).
41. D. M. Del Valle *et al.*, An inflammatory cytokine signature predicts COVID-19 severity and survival. *Nature Medicine* **26**, 1636-1643 (2020).
42. Y. Lee *et al.*, Induction and molecular signature of pathogenic TH17 cells. *Nat Immunol* **13**, 991-999 (2012).
43. Z. A. Rizvi *et al.*, Golden Syrian hamster as a model to study cardiovascular complications associated with SARS-CoV-2 infection. *eLife* **11**, e73522 (2022).
44. M. DuPage, J. A. Bluestone, Harnessing the plasticity of CD4+ T cells to treat immune-mediated disease. *Nature Reviews Immunology* **16**, 149-163 (2016).
45. S. K. Wculek, S. C. Khouili, E. Priego, I. Heras-Murillo, D. Sancho, Metabolic Control of Dendritic Cell Functions: Digesting Information. *Frontiers in Immunology* **10**, (2019).
46. L. Ansone *et al.*, Amino Acid Metabolism is Significantly Altered at the Time of Admission in Hospital for Severe COVID-19 Patients: Findings from Longitudinal Targeted Metabolomics Analysis. *Microbiology Spectrum* **9**, e00338-00321 (2021).
47. V. Bronte, P. Zanovello, Regulation of immune responses by L-arginine metabolism. *Nature Reviews Immunology* **5**, 641-654 (2005).
48. A. Swain *et al.*, Comparative evaluation of itaconate and its derivatives reveals divergent inflammasome and type I interferon regulation in macrophages. *Nature Metabolism* **2**, 594-602 (2020).
49. E. L. Mills *et al.*, itaconate is an anti-inflammatory metabolite that activates Nrf2 via alkylation of KEAP1. *Nature* **556**, 113-117 (2018).
50. E. H. Kobayashi *et al.*, Nrf2 suppresses macrophage inflammatory response by blocking proinflammatory cytokine transcription. *Nature Communications* **7**, 11624 (2016).
51. J. S. Maras *et al.*, Multi-omics analysis of respiratory specimen characterizes baseline molecular determinants associated with SARS-CoV-2 outcome. *iScience* **24**, 102823 (2021).
52. K. U. Schallreuter, J. W. Wood, A possible mechanism of action for azelaic acid in the human epidermis. *Archives of Dermatological Research* **282**, 168-171 (1990).

Figures and Figure legends

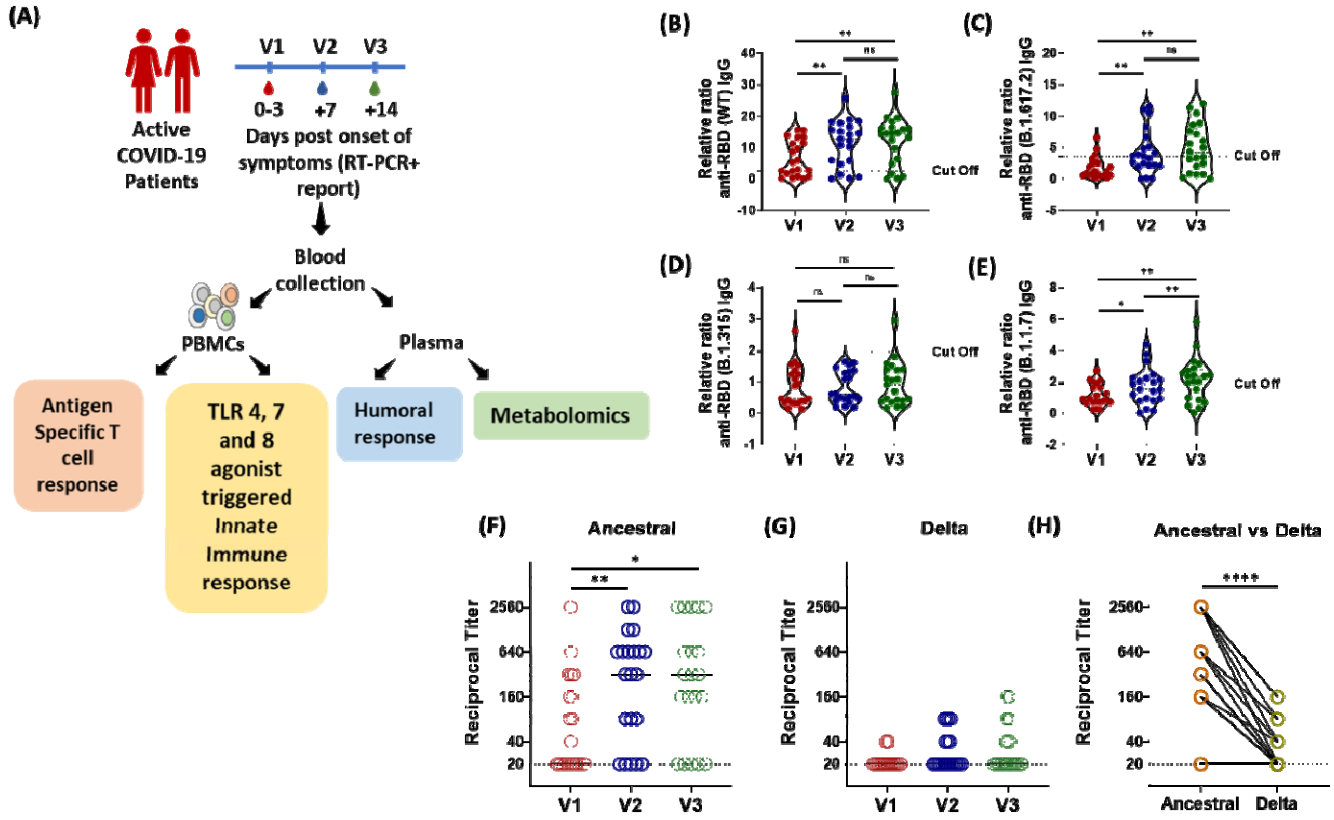

Fig 1: Longitudinal Analysis of Humoral Immune Response against the SARS-CoV-2 during acute COVID-19 infection. (A) Schematic experimental design and longitudinal sample collection at specific time intervals after confirmed SARS-CoV-2 infection in mildly infected patients. **(B-E)** The longitudinal anti-RBD IgG responses were evaluated by performing ELISA against the RBD proteins of **(B)** WT (Wuhan isolate) **(C)** Delta (B.1.617.2) **(D)** Beta (B.1.315) **(E)** Alpha (B.1.1.7). All data, represented as ratio-converted ELISA reads to a pool of pre-pandemic negative control samples (relative ratio), were plotted using violin plots.

(F-H) The longitudinal neutralizing antibody titers against **(F)** the ancestral strain and **(G)** the delta strain of SARS-CoV-2 during V1 (day 0-3), V2 (day 7) and V3 (day 14) from COVID-19 positivity **(H)** The paired representation of NAb titers in the active COVID-19 patients during V3 against the ancestral and delta variants of SARS-CoV-2.

The dots represent each individual sample. Tukey's multiple comparisons and two-sided Wilcoxon Signed Rank tests were employed for unpaired and paired analysis, respectively. n.s = not significant, *= $p \leq 0.05$, **= $p \leq 0.01$, **** = $p < 0.0001$.

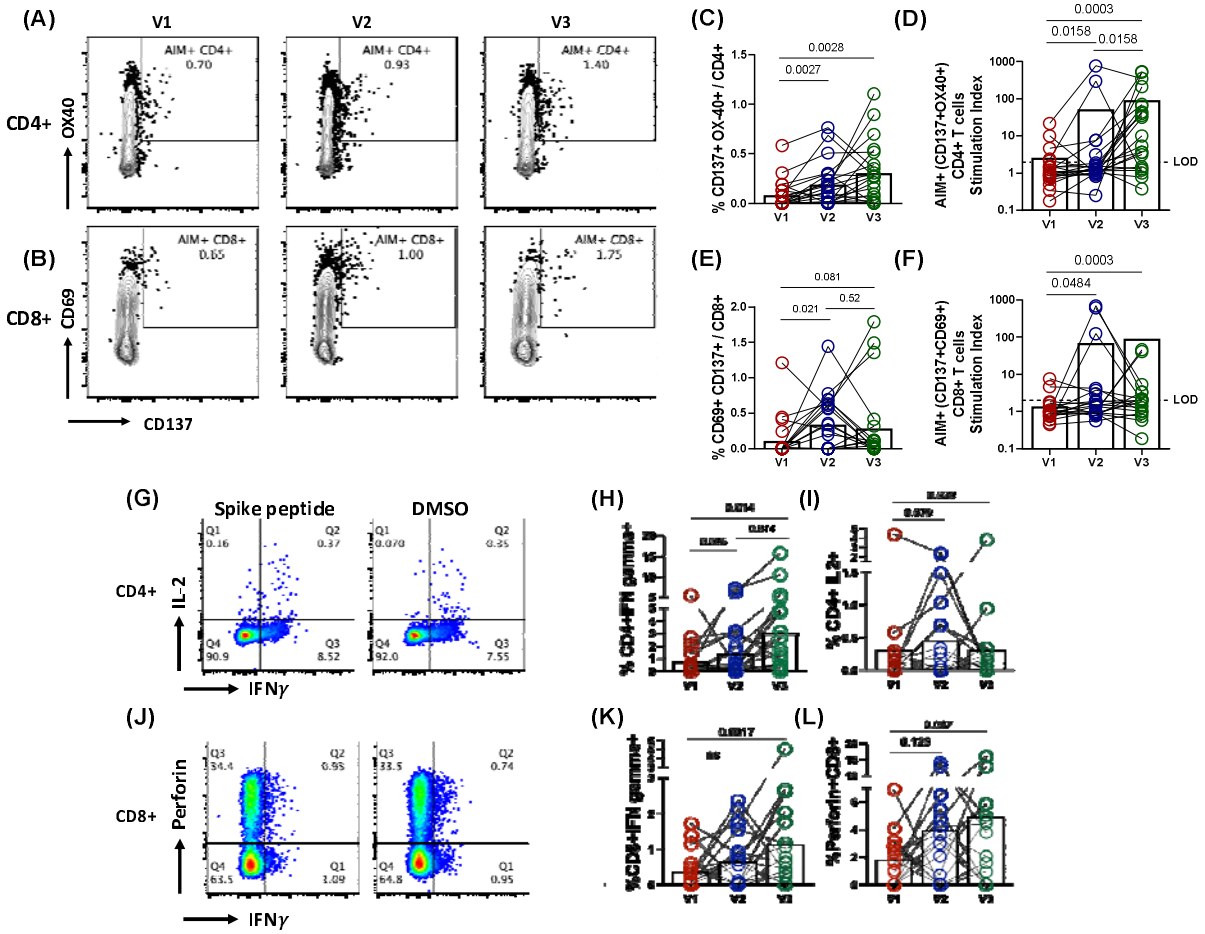

Fig. 2. Longitudinal dynamics of antigen-specific T cell immune responses during COVID-19 infection. Representative flow cytometry plots of SARS-CoV-2 Spike specific T cells expressing activation-induced markers (AIM) **(A)** CD4+ (CD137+OX40+) **(B)** CD8+ (CD137+CD69+); **(C-F)** Longitudinal analysis of the AIM response in paired samples from the same subject **(C)** percentage frequency of CD4+AIM+ cells **(D)** Stimulation index (SI) of CD4+ AIM+ cells **(E)** %frequency of CD8+AIM+ cells **(F)** SI of CD8+ AIM+ cells.

(G, J) Representative flow cytometry plots for the intracellular cytokine staining (ICS) assay of cells upon stimulation with spike peptide pool compared to the DMSO; Longitudinal analysis of the frequency (percentage of total CD4+ or CD8+ cells) of cytokine+ cells in paired samples from the same subject. **(H)** CD4+ Interferon gamma (IFNγ) **(I)** CD4+ Interleukin 2 **(K)** CD8+ Interferon gamma **(L)** CD8+ Perforin; Each datapoint shown is background subtracted, and bars represent mean values for each time point. Two-sided Wilcoxon Signed Rank tests were employed for paired analysis. LOD = Limit of detection for AIM assay was SI<2.

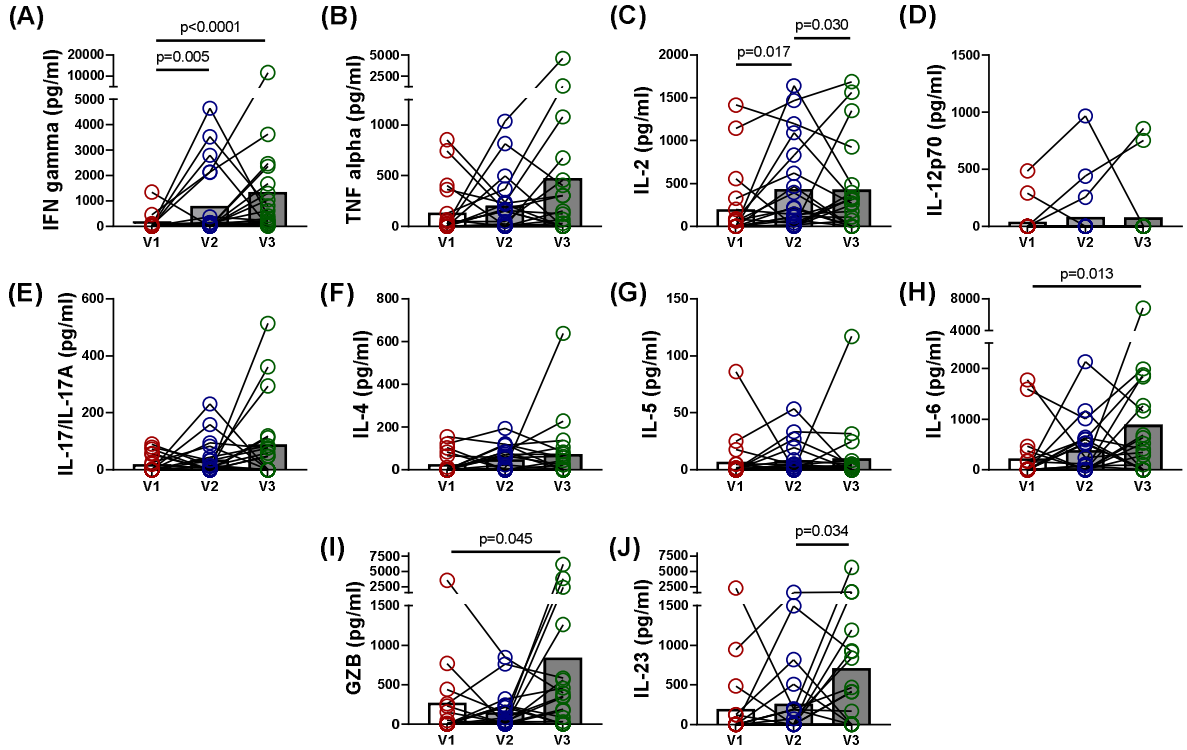

Fig. 3. Longitudinal dynamics of antigen-specific cytokine release by PBMCs during COVID-19 infection. Graphs represent longitudinal cytokine released by paired PBMC samples from the same subject upon stimulation with SARS-CoV-2 spike peptide pool for 18-20h. Each dot represents an individual sample, and the paired samples were analyzed using the two-sided Wilcoxon Signed Rank test. Bars represent mean values.

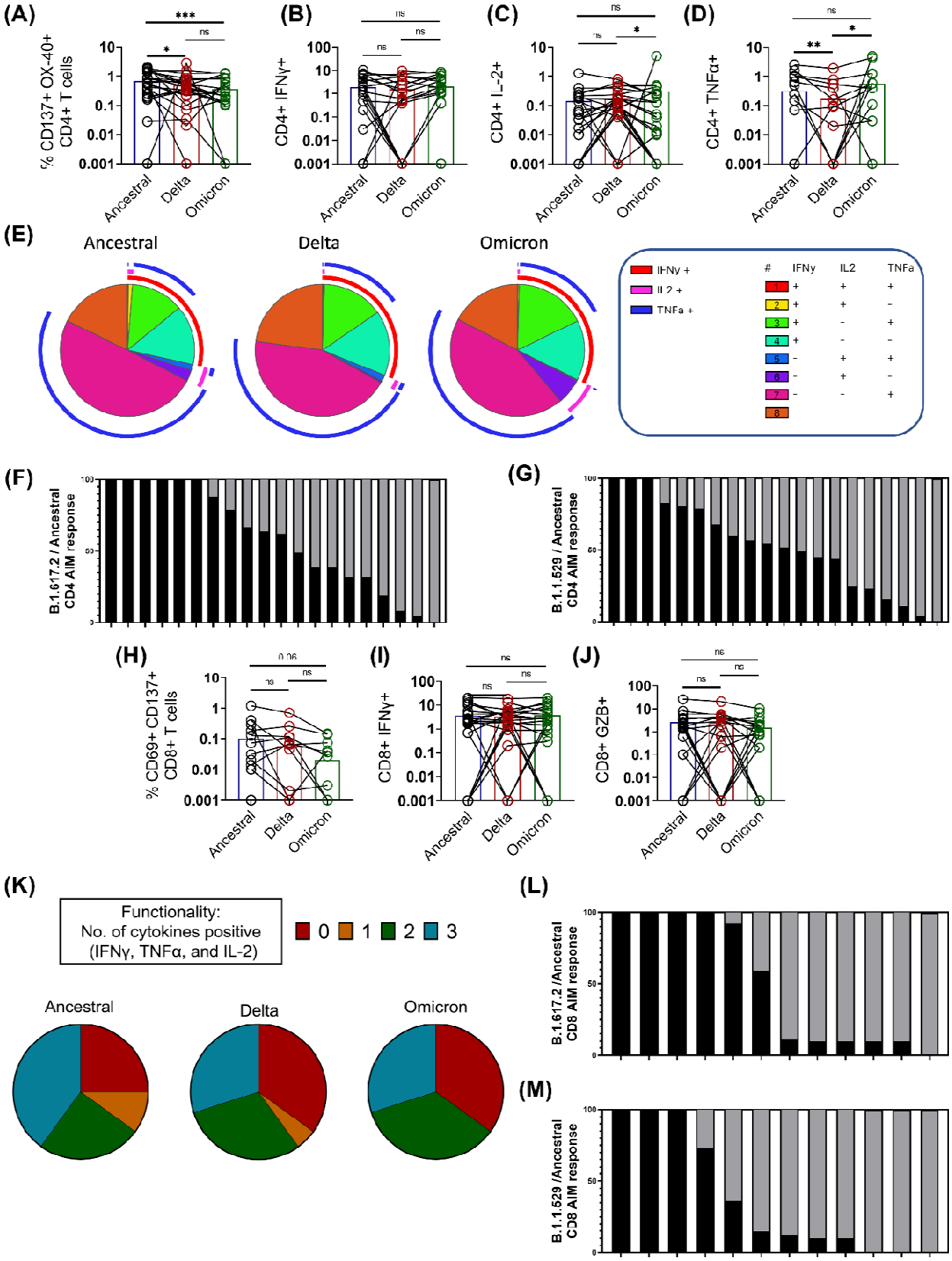
(A)
% CD137+ OX-40+ CD4+ T cells
(B)
CD4+ IFNγ+
(C)
CD4+ IL-2+
(D)
CD4+ TNFα+
Ancestral
Delta
Omicron
(E)
Ancestral
Delta
Omicron
IFNγ +
IL 2 +
TNFa +
IFNy IL2 TNFa
(F)
B.1.617.2 / Ancestral CD4 AIM response
(G)
B.1.1.529 / Ancestral CD4 AIM response
(H)
% CD69+ CD137+ CD8+ T cells
(I)
CD8+ IFNγ+
(J)
CD8+ GZB+
(K)
Functionality:
No. of cytokines positive
(IFNγ, TNFα, and IL-2)
0 1 2 3
Ancestral
Delta
Omicron
(L)
B.1.617.2 /Ancestral CD8 AIM response
(M)
B.1.1.529 /Ancestral CD8 AIM response

497

Fig. 4. Cross-reactive CD4+ and CD8+ T cell response against Delta and Omicron Spike in acute COVID-19 patients. Spike-specific T cell responses in selected samples of active COVID-19 patients (n=24) were simultaneously tested for reactivity against spike peptide pools of WT (Ancestral), Delta (B.1.617.2), and Omicron (B.1.1.529). **(A-D)** Frequencies of antigen-specific CD4+ T cell responses **(A)** CD4+ AIM [CD137+OX40+] **(B)** CD4+ IFNγ **(C)** CD4+ IL2 **(D)** CD4+ TNFα. **(E)** Pie charts showing the mean frequency for each combination of functional profiles of AIM+ CD4 T cell responses in active COVID-19 individuals;

Cross-reactive CD4 AIM responses described on a singular basis as **(F)** percentage B.1.617.2/wild-type **(G)** percentage B.1.1.529/wildtype.

(H-J) Frequencies of antigen-specific CD8+ T cell responses **(H)** CD8+ AIM [CD137+CD69+] **(I)** CD8+ IFNγ **(J)** CD8+Granzyme B **(K)** Poly-functional response calculated for an individual sample that is positive for the number of antigen-specific cytokine functions detected;

Cross-reactive CD8 AIM responses described on a singular basis as **(L)** percentage B.1.617.2/wild-type **(M)** percentage B.1.1.529/wildtype.

Bars represent mean values, each dot represents an individual sample, and the solid line connects the same sample stimulated with different peptide pools. AIM, activation-induced markers; GZB, granzyme B; ns, non-significant

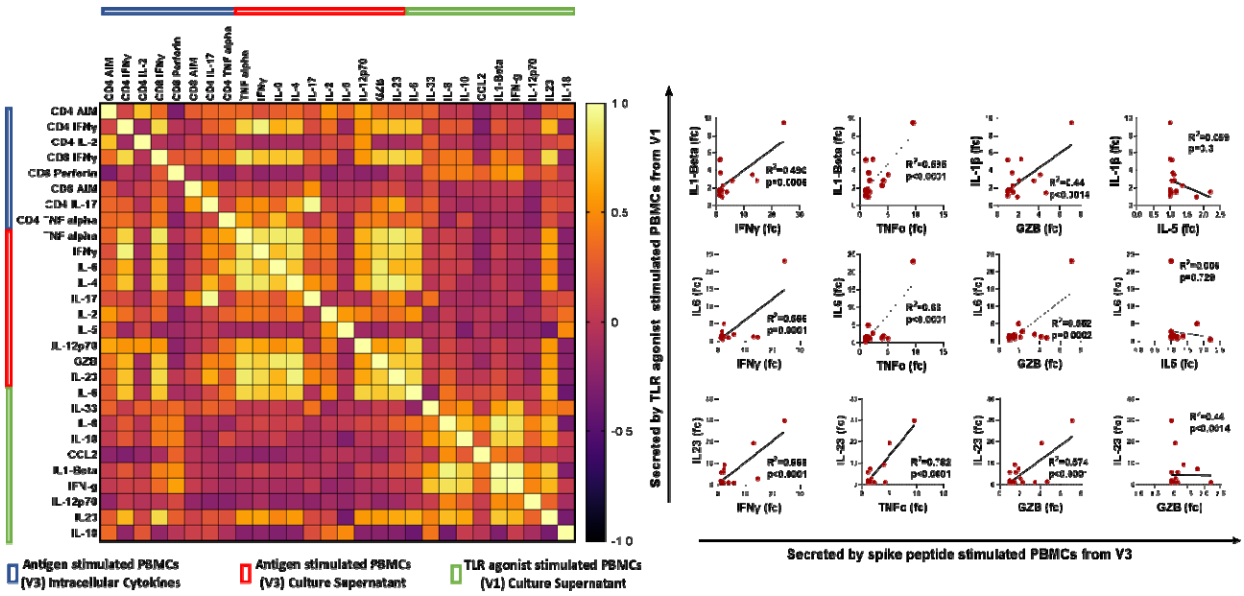

Fig.5. Correlation of early innate immune responses with adaptive immune responses in active COVID-19 patients. Correlation between the cytokine released upon TLR agonist stimulation of PBMCs from early stages of COVID-19 infection (V1) and the magnitude of antigen-specific T cell responses during the later stages of COVID-19 disease (V3). The responses were calculated as fold change in the stimulated wells compared to the unstimulated wells **(A)** A heatmap of correlation analysis; the blue rectangle depicts the analysis of stimulated PBMCs using flow cytometry; the red rectangle represents the fold change of cytokines released in the culture supernatant upon peptide stimulation; and the green rectangle represents the fold change of cytokines released in the culture supernatant upon stimulation with TLR agonists: poly I:C (25 µg/ml) and R848 (4 µg/ml) for 24h. **(B)** XY correlation plots where the y axis represents the fold change of cytokines secreted upon TLR agonist stimulation of PBMCs from V1 and the x-axis represents the fold change of cytokines secreted upon peptide pool stimulation of PBMCs from V3. Pearson correlation coefficient is indicated. fc, fold change; GZB, granzyme B

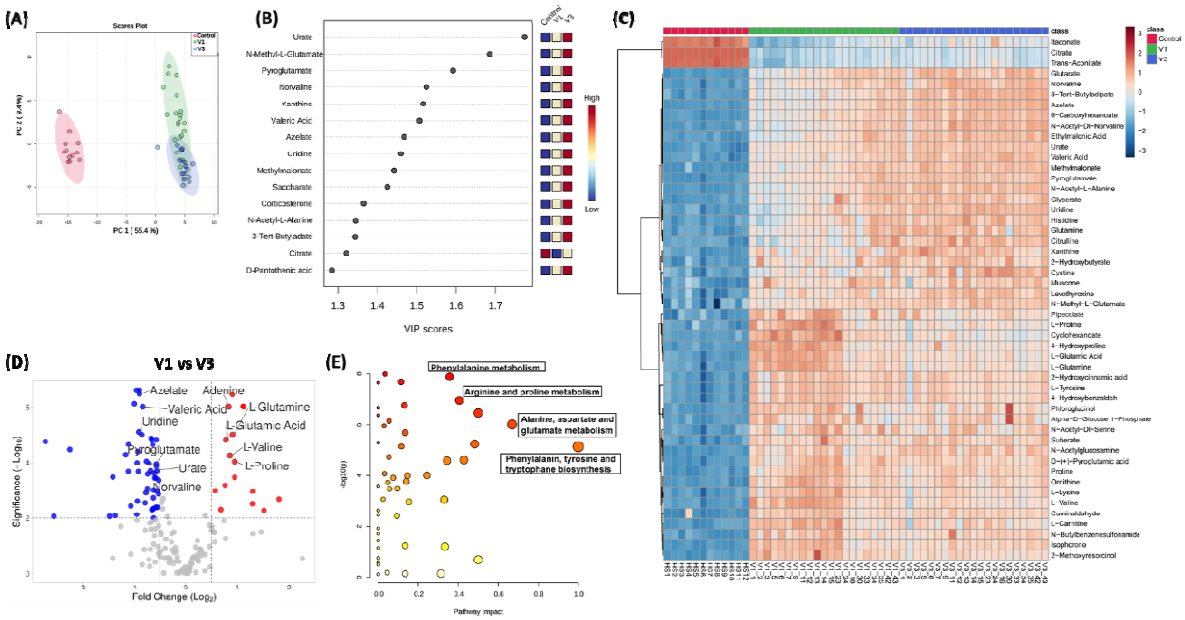

Fig 6. Metabolomic analysis of SARS-CoV-2 patient plasma samples compared to age-matched healthy controls. (A) Principal Component Analysis of the untargeted metabolites of the three groups **(B)** Important features identified by PLS-DA. The colored boxes indicate relative concentrations of designated metabolites in each study group. **(C)** hierarchical cluster analysis is shown as a heatmap of top 50 metabolites (FDR<0.05) **(D)** Pathway enrichment analysis using KEGG of all the metabolites (n=158) that are significantly altered during COVID-19 infection. **(E)** Volcano plot comparing the significantly changed (p=0.001, FC>1.5) metabolites during the early (V1) and later stages of disease (V3).

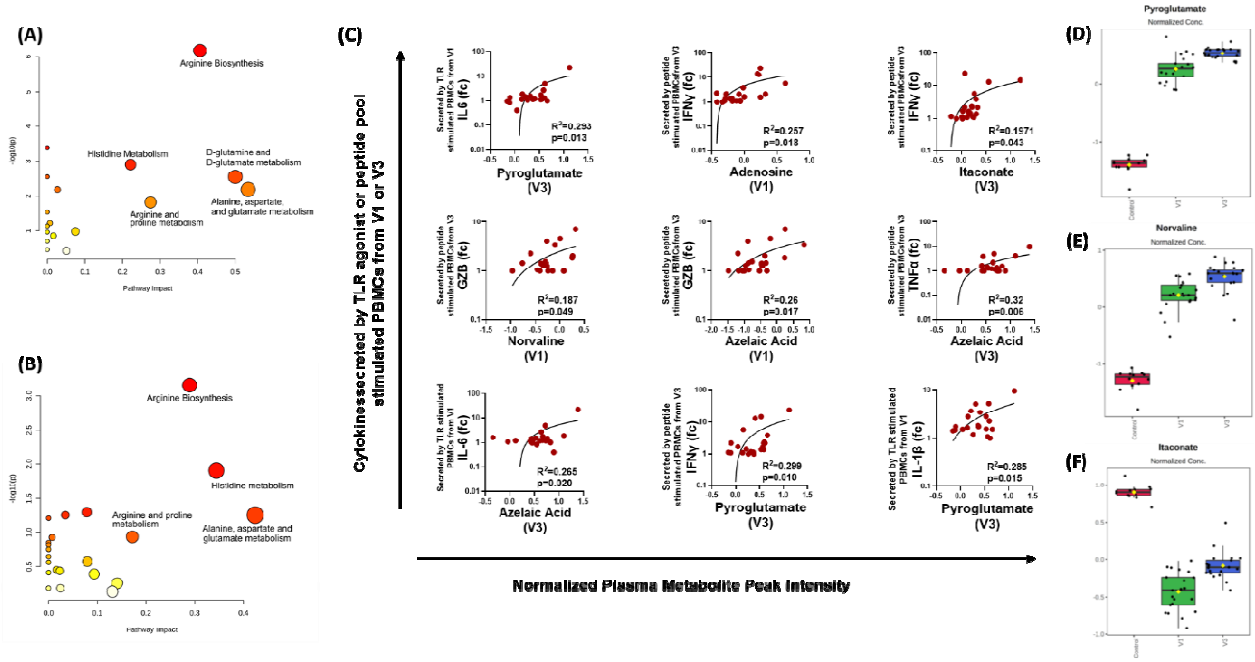

Fig. 7. Correlation of metabolites with immune responses. Pathway analysis of plasma metabolites that significantly correlated (r>0.5, p<0.05) with **(A)** the innate immune response (V1) and **(B)** the T cell immune response (V3) **(C)** Representative correlation plots of metabolites from V1 and V3 that correlate with the cytokine release responses from TLR stimulated innate, and peptide pool stimulated adaptive immune responses. **(D-F)** Normalized concentrations of metabolites at the three-time points **(D)** Pyroglutamate **(E)** Norvaline **(F)** Itaconate. Each dot represents an individual sample. The bold black line represents the median values. The box represents the interquartile range. The vertical line represents the range of normalized values of the peak intensities of the metabolites estimated by mass spectrometry. Pearson correlation coefficient is indicated. GZB, granzyme B

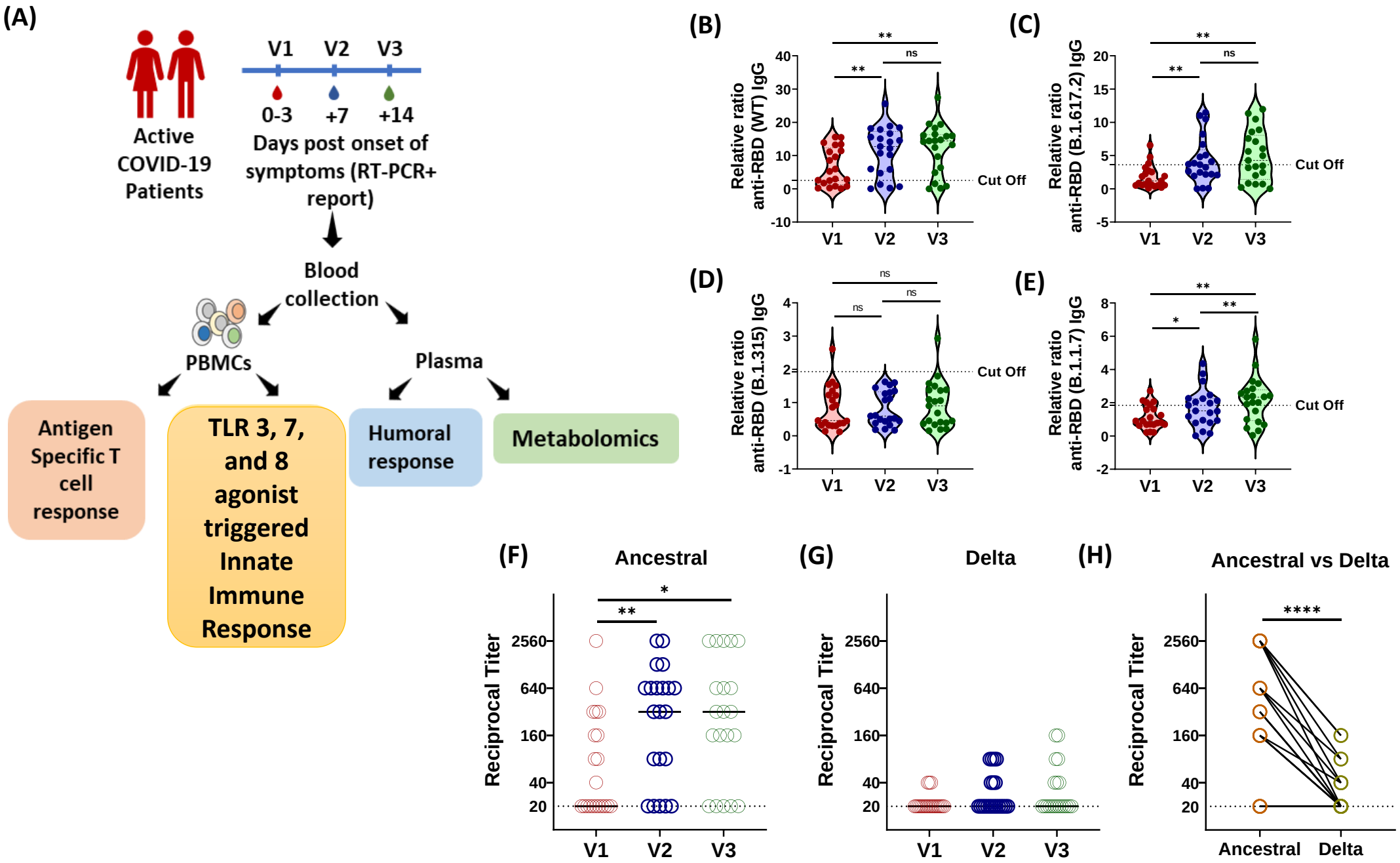
(A)
Active COVID-19 Patients
V1 V2 V3
0-3 +7 +14
Days post onset of symptoms (RT-PCR+ report)
Blood collection
PBMCs
Plasma
Antigen Specific T cell response
TLR 3, 7, and 8 agonist triggered Innate Immune Response
Humoral response
Metabolomics
(B)
Relative ratio anti-RBD (WT) IgG
Cut Off
(C)
Relative ratio anti-RBD (B.1.617.2) IgG
Cut Off
(D)
Relative ratio anti-RBD (B.1.315) IgG
Cut Off
(E)
Relative ratio anti-RBD (B.1.1.7) IgG
Cut Off
V1 V2 V3
(F) Ancestral
(G) Delta
(H) Ancestral vs Delta
Reciprocal Titer
Ancestral Delta

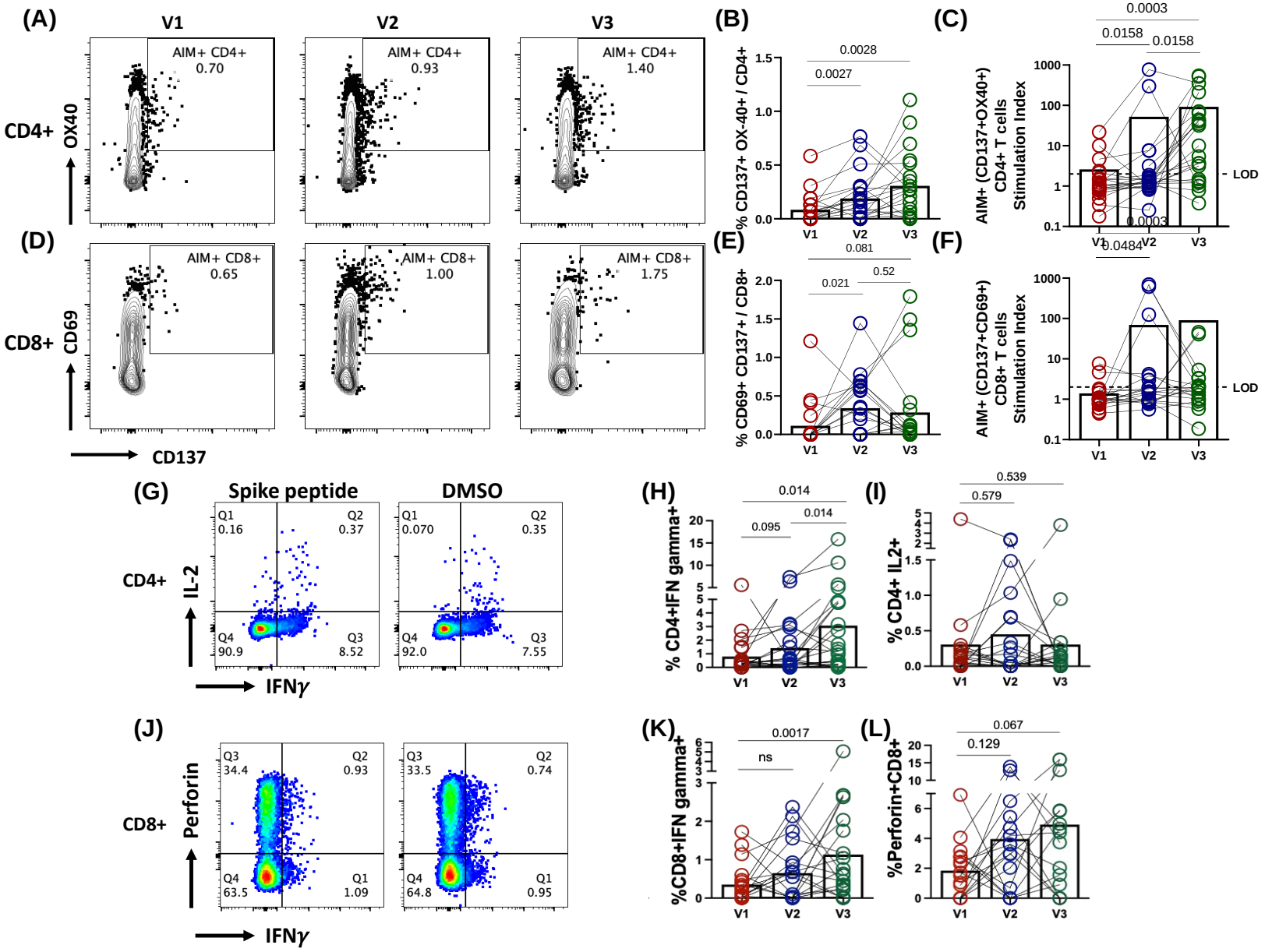
(A)
V1
V2
V3
CD4+
OX40
AIM+ CD4+
0.70
AIM+ CD4+
0.93
AIM+ CD4+
1.40
(B)
% CD137+ OX-40+ / CD4+
0.0028
0.0027
(C)
AIM+ (CD137+OX40+) CD4+ T cells Stimulation Index
0.0003
0.0158
0.0158
0.0003
0.0484
LOD
(D)
CD8+
CD69
CD137
AIM+ CD8+
0.65
AIM+ CD8+
1.00
AIM+ CD8+
1.75
(E)
% CD69+ CD137+ / CD8+
0.081
0.021
0.52
(F)
AIM+ (CD137+CD69+) CD8+ T cells Stimulation Index
LOD
(G)
Spike peptide
DMSO
CD4+
IL-2
IFNγ
Q1 0.16
Q2 0.37
Q4 90.9
Q3 8.52
Q1 0.070
Q2 0.35
Q4 92.0
Q3 7.55
(H)
% CD4+IFN gamma+
0.014
0.014
0.095
(I)
% CD4+ IL2+
0.539
0.579
(J)
CD8+
Perforin
IFNγ
Q3 34.4
Q2 0.93
Q4 63.5
Q1 1.09
Q3 33.5
Q2 0.74
Q4 64.8
Q1 0.95
(K)
%CD8+IFN gamma+
0.0017
ns
(L)
%Perforin+CD8+
0.067
0.129
V1
V2
V3

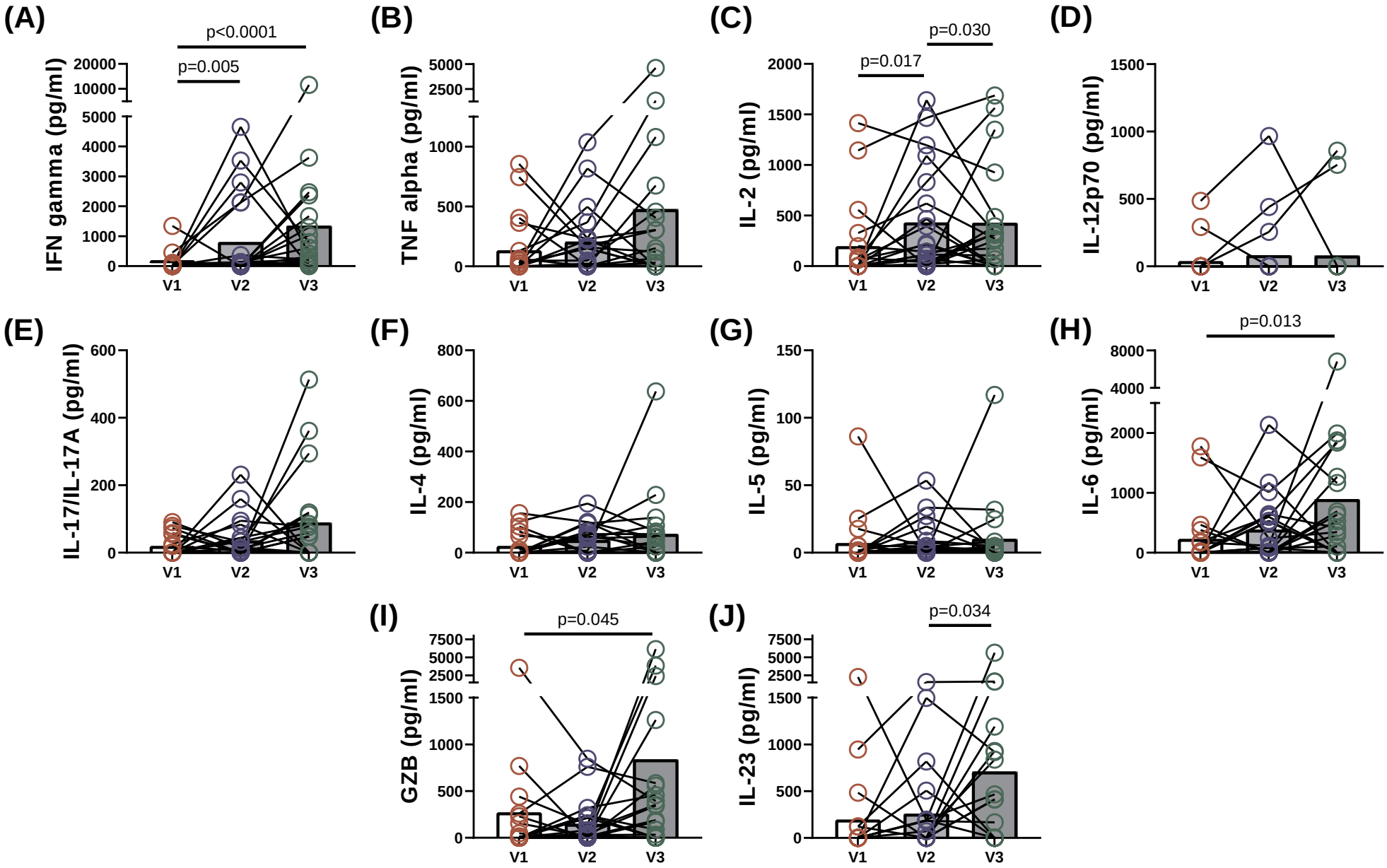
(A)
p<0.0001
p=0.005
IFN gamma (pg/ml)
20000
10000
5000
4000
3000
2000
1000
0
V1
V2
V3
(B)
TNF alpha (pg/ml)
5000
2500
1000
500
0
V1
V2
V3
(C)
p=0.030
p=0.017
IL-2 (pg/ml)
2000
1500
1000
500
0
V1
V2
V3
(D)
IL-12p70 (pg/ml)
1500
1000
500
0
V1
V2
V3
(E)
IL-17/IL-17A (pg/ml)
600
400
200
0
V1
V2
V3
(F)
IL-4 (pg/ml)
800
600
400
200
0
V1
V2
V3
(G)
IL-5 (pg/ml)
150
100
50
0
V1
V2
V3
(H)
p=0.013
IL-6 (pg/ml)
8000
4000
2000
1000
0
V1
V2
V3
(I)
p=0.045
GZB (pg/ml)
7500
5000
2500
1500
1000
500
0
V1
V2
V3
(J)
p=0.034
IL-23 (pg/ml)
7500
5000
2500
1500
1000
500
0
V1
V2
V3

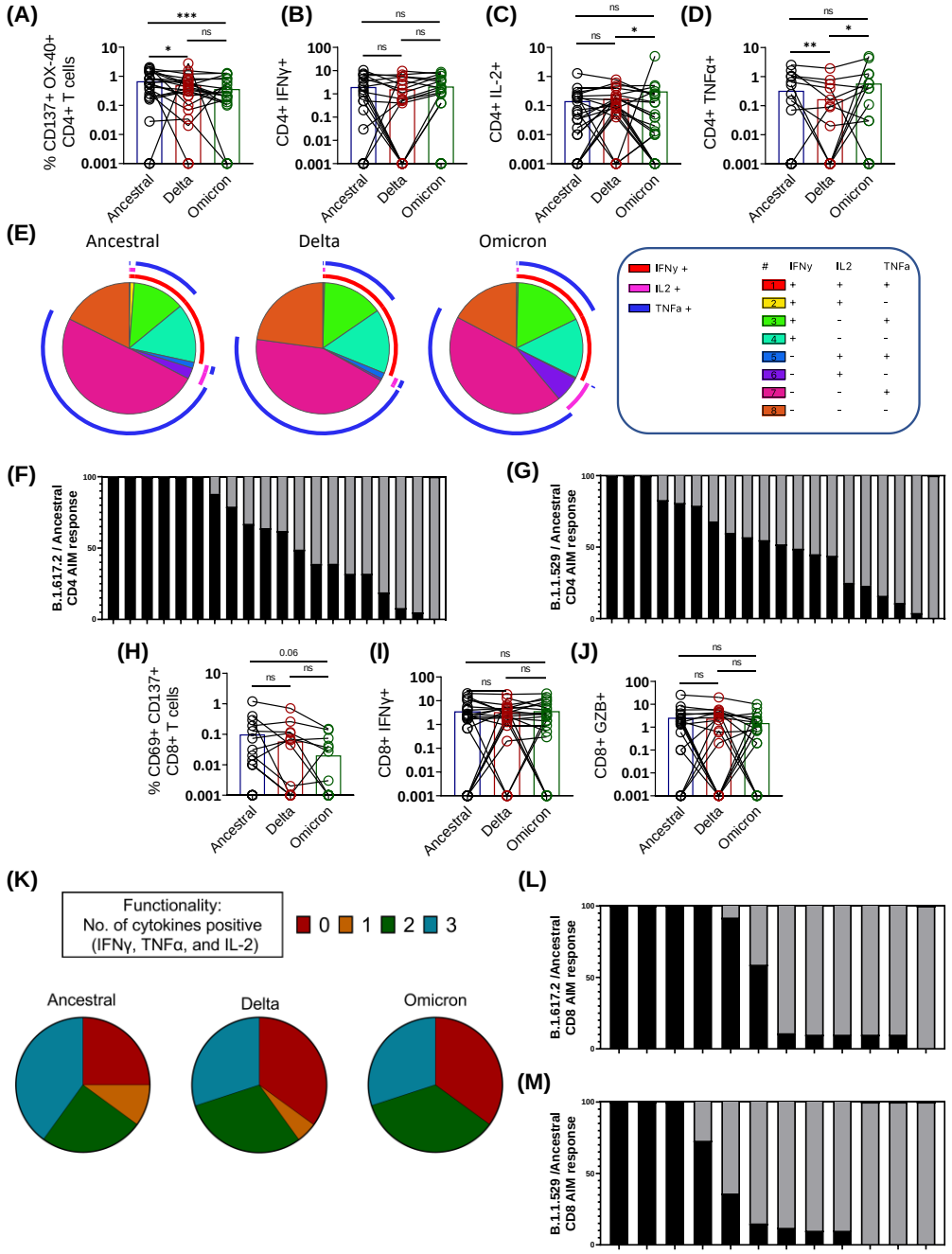
(A)
% CD137+ OX-40+ CD4+ T cells
(B)
CD4+ IFNγ+
(C)
CD4+ IL-2+
(D)
CD4+ TNFα+
Ancestral
Delta
Omicron
(E)
Ancestral
Delta
Omicron
IFNγ +
IL2 +
TNFa +
IFNγ IL2 TNFa
1 + + +
2 + + -
3 + - +
4 + - -
5 - + +
6 - + -
7 - - +
8 - - -
(F)
B.1.617.2 / Ancestral CD4 AIM response
(G)
B.1.1.529 / Ancestral CD4 AIM response
(H)
% CD69+ CD137+ CD8+ T cells
(I)
CD8+ IFNγ+
(J)
CD8+ GZB+
(K)
Functionality: No. of cytokines positive (IFNγ, TNFα, and IL-2)
0 1 2 3
Ancestral
Delta
Omicron
(L)
B.1.617.2 /Ancestral CD8 AIM response
(M)
B.1.1.529 /Ancestral CD8 AIM response

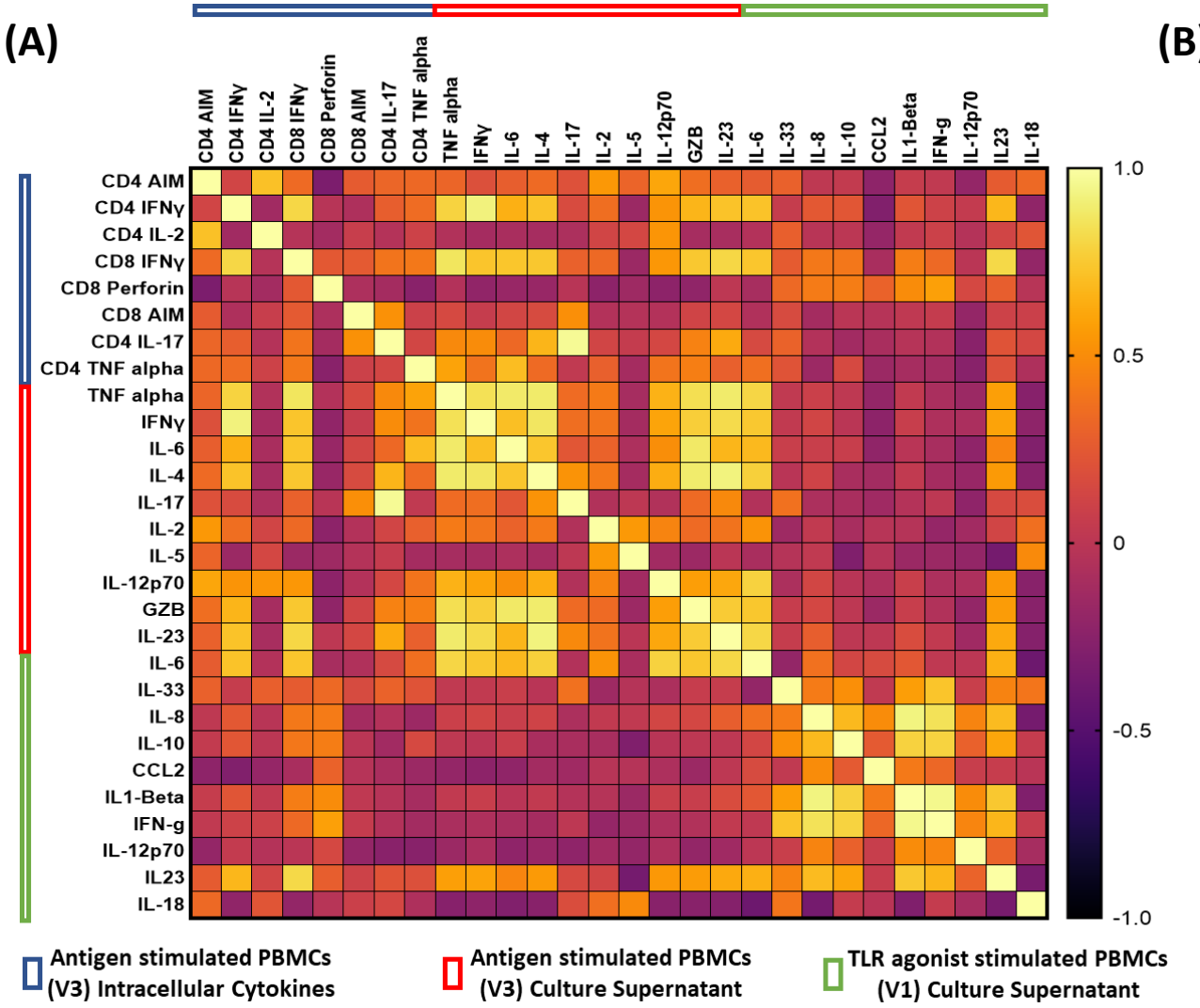
(A)
CD4 AIM
CD4 IFNγ
CD4 IL-2
CD8 IFNγ
CD8 Perforin
CD8 AIM
CD4 IL-17
CD4 TNF alpha
TNF alpha
IFNγ
IL-6
IL-4
IL-17
IL-2
IL-5
IL-12p70
GZB
IL-23
IL-6
IL-33
IL-8
IL-10
CCL2
IL1-Beta
IFN-g
IL-12p70
IL23
IL-18
1.0
0.5
0
-0.5
-1.0
Antigen stimulated PBMCs (V3) Intracellular Cytokines
Antigen stimulated PBMCs (V3) Culture Supernatant
TLR agonist stimulated PBMCs (V1) Culture Supernatant

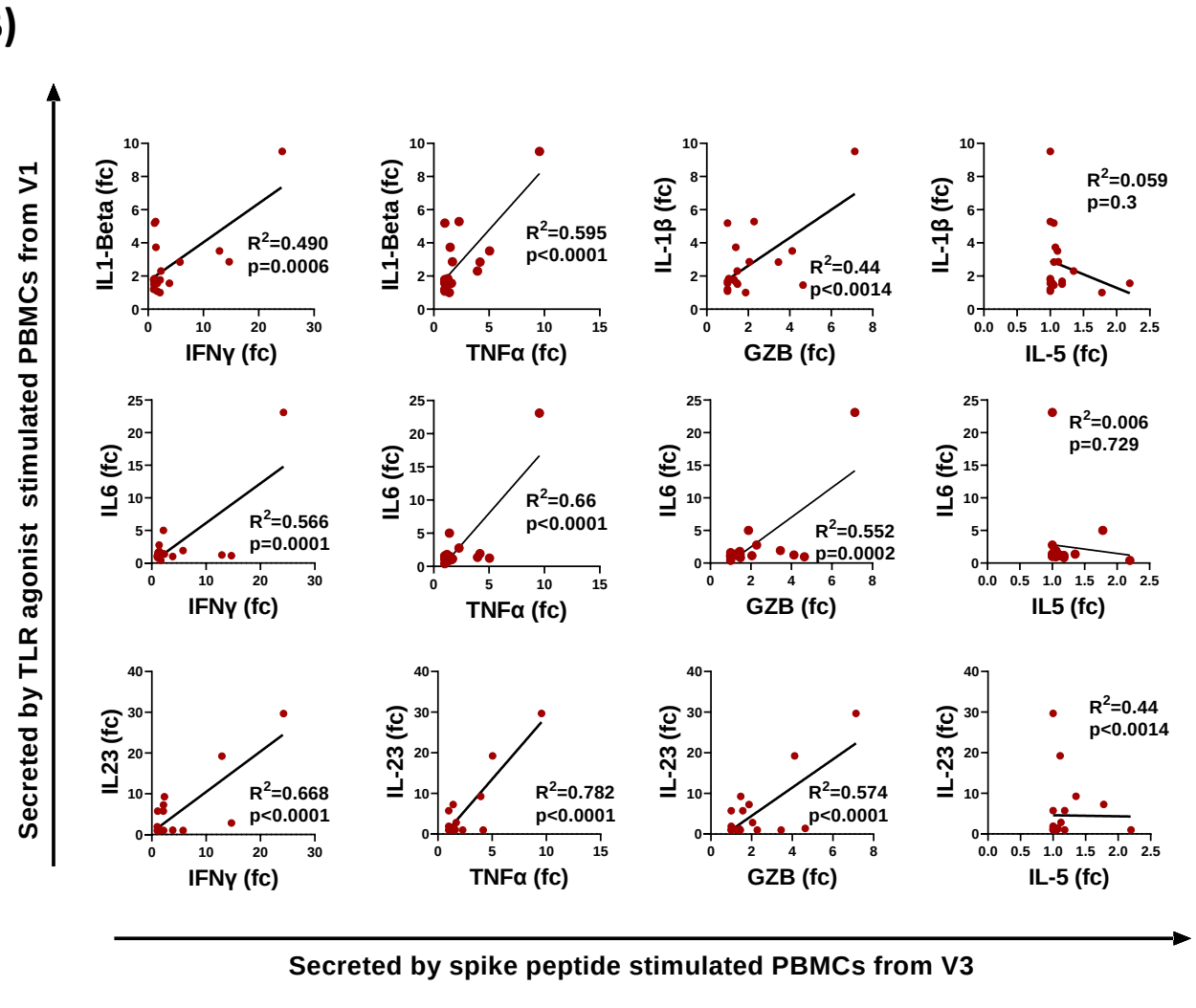
(B)
Secreted by TLR agonist stimulated PBMCs from V1
IL1-Beta (fc)
IFNγ (fc)
R2=0.490
p=0.0006
IL1-Beta (fc)
TNFα (fc)
R2=0.595
p<0.0001
IL-1β (fc)
GZB (fc)
R2=0.44
p<0.0014
IL-1β (fc)
IL-5 (fc)
R2=0.059
p=0.3
IL6 (fc)
IFNγ (fc)
R2=0.566
p=0.0001
IL6 (fc)
TNFα (fc)
R2=0.66
p<0.0001
IL6 (fc)
GZB (fc)
R2=0.552
p=0.0002
IL6 (fc)
IL5 (fc)
R2=0.006
p=0.729
IL23 (fc)
IFNγ (fc)
R2=0.668
p<0.0001
IL-23 (fc)
TNFα (fc)
R2=0.782
p<0.0001
IL-23 (fc)
GZB (fc)
R2=0.574
p<0.0001
IL-23 (fc)
IL-5 (fc)
R2=0.44
p<0.0014
Secreted by spike peptide stimulated PBMCs from V3

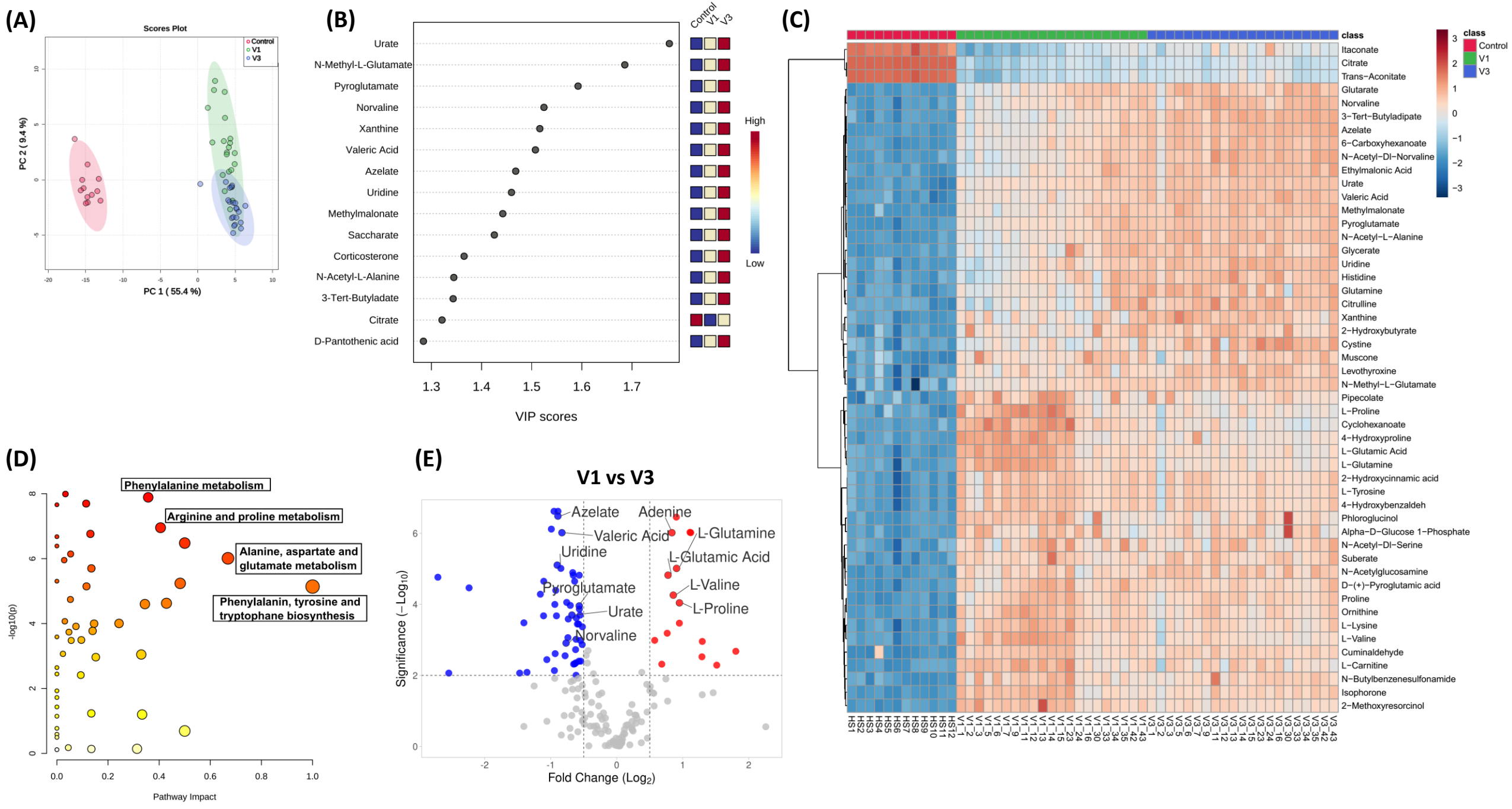
(A)
Scores Plot
Control
V1
V3
PC 2 (9.4 %)
PC 1 (55.4 %)
(B)
Control
V1
V3
Urate
N-Methyl-L-Glutamate
Pyroglutamate
Norvaline
Xanthine
Valeric Acid
Azelate
Uridine
Methylmalonate
Saccharate
Corticosterone
N-Acetyl-L-Alanine
3-Tert-Butyladate
Citrate
D-Pantothenic acid
High
Low
1.3
1.4
1.5
1.6
1.7
VIP scores
(C)
class
Control
V1
V3
Itaconate
Citrate
Trans-Aconitate
Glutarate
Norvaline
3-Tert-Butyladipate
Azelate
6-Carboxyhexanoate
N-Acetyl-Dl-Norvaline
Ethylmalonic Acid
Urate
Valeric Acid
Methylmalonate
Pyroglutamate
N-Acetyl-L-Alanine
Glycerate
Uridine
Histidine
Glutamine
Citrulline
Xanthine
2-Hydroxybutyrate
Cystine
Muscone
Levothyroxine
N-Methyl-L-Glutamate
Pipecolate
L-Proline
Cyclohexanoate
4-Hydroxyproline
L-Glutamic Acid
L-Glutamine
2-Hydroxycinnamic acid
L-Tyrosine
4-Hydroxybenzaldeh
Phloroglucinol
Alpha-D-Glucose 1-Phosphate
N-Acetyl-Dl-Serine
Suberate
N-Acetylglucosamine
D-(+)-Pyroglutamic acid
Proline
Ornithine
L-Lysine
L-Valine
Cuminaldehyde
L-Carnitine
N-Butylbenzenesulfonamide
Isophorone
2-Methoxyresorcinol
(D)
Phenylalanine metabolism
Arginine and proline metabolism
Alanine, aspartate and glutamate metabolism
Phenylalanin, tyrosine and tryptophane biosynthesis
-log10(p)
Pathway Impact
(E)
V1 vs V3
Azelate
Adenine
Valeric Acid
L-Glutamine
Uridine
L-Glutamic Acid
Pyroglutamate
L-Valine
Urate
L-Proline
Norvaline
Significance (−Log10)
Fold Change (Log2)

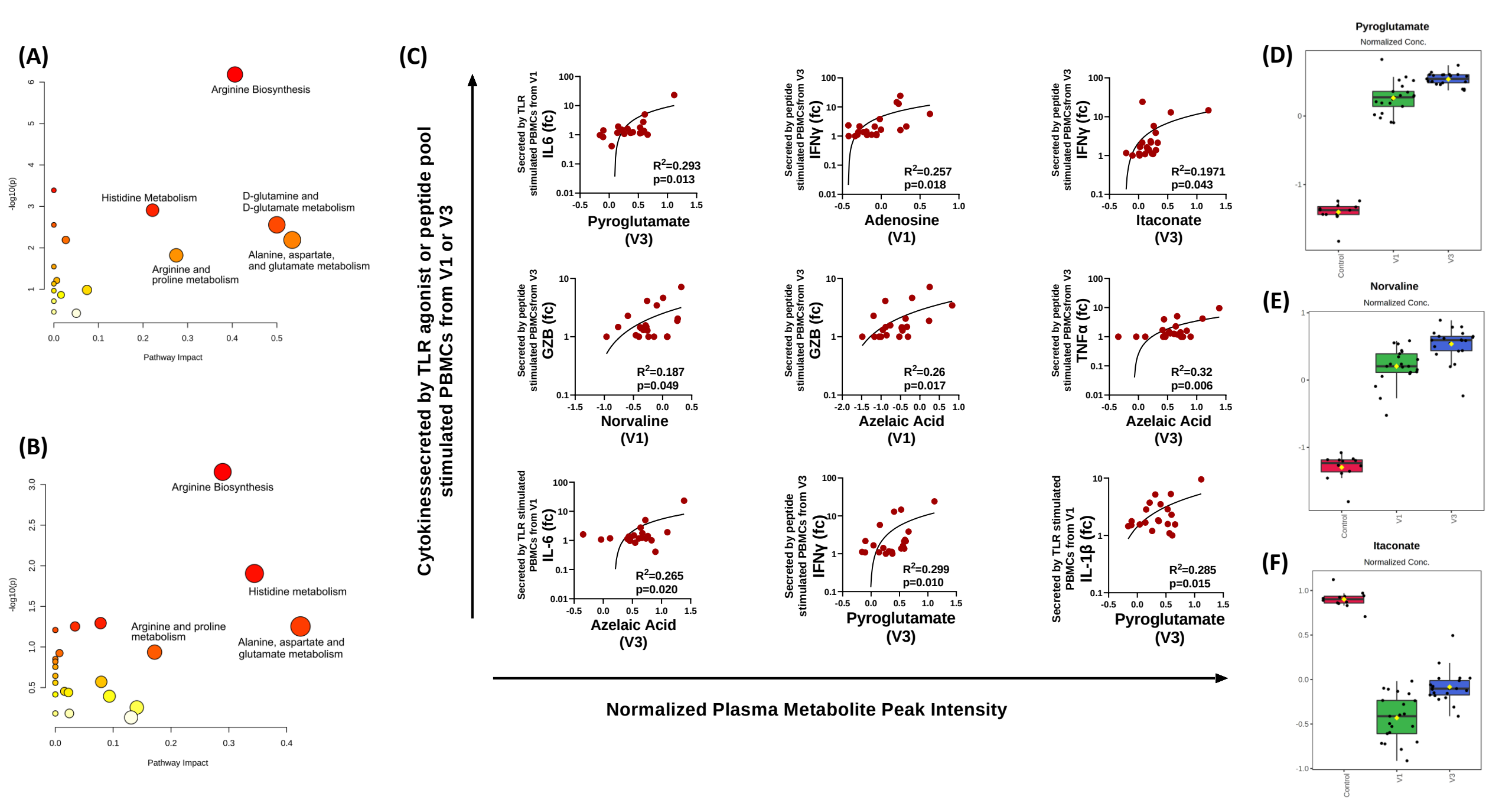
(A)
Arginine Biosynthesis
Histidine Metabolism
D-glutamine and D-glutamate metabolism
Arginine and proline metabolism
Alanine, aspartate, and glutamate metabolism
-log10(p)
Pathway Impact
(B)
Arginine Biosynthesis
Histidine metabolism
Arginine and proline metabolism
Alanine, aspartate and glutamate metabolism
-log10(p)
Pathway Impact
(C)
Cytokinessecreted by TLR agonist or peptide pool stimulated PBMCs from V1 or V3
Secreted by TLR stimulated PBMCs from V1 IL6 (fc)
Pyroglutamate (V3)
R2=0.293 p=0.013
Secreted by peptide stimulated PBMCsfrom V3 IFNγ (fc)
Adenosine (V1)
R2=0.257 p=0.018
Secreted by peptide stimulated PBMCsfrom V3 IFNγ (fc)
Itaconate (V3)
R2=0.1971 p=0.043
Secreted by peptide stimulated PBMCsfrom V3 GZB (fc)
Norvaline (V1)
R2=0.187 p=0.049
Secreted by peptide stimulated PBMCsfrom V3 GZB (fc)
Azelaic Acid (V1)
R2=0.26 p=0.017
Secreted by peptide stimulated PBMCsfrom V3 TNFα (fc)
Azelaic Acid (V3)
R2=0.32 p=0.006
Secreted by TLR stimulated PBMCs from V1 IL-6 (fc)
Azelaic Acid (V3)
R2=0.265 p=0.020
Secreted by peptide stimulated PBMCs from V3 IFNγ (fc)
Pyroglutamate (V3)
R2=0.299 p=0.010
Secreted by TLR stimulated PBMCs from V1 IL-1β (fc)
Pyroglutamate (V3)
R2=0.285 p=0.015
Normalized Plasma Metabolite Peak Intensity
(D)
Pyroglutamate
Normalized Conc.
Control
V1
V3
(E)
Norvaline
Normalized Conc.
Control
V1
V3
(F)
Itaconate
Normalized Conc.
Control
V1
V3